

AD-766 650

SEEK STORM RADAR SENSITIVITY STUDY

MITRE CORP.

PREPARED FOR  
AIR FORCE SYSTEMS COMMAND

AUGUST 1973

DISTRIBUTED BY:

**NTIS**

National Technical Information Service  
U. S. DEPARTMENT OF COMMERCE

SEEK STORM RADAR SENSITIVITY STUDY

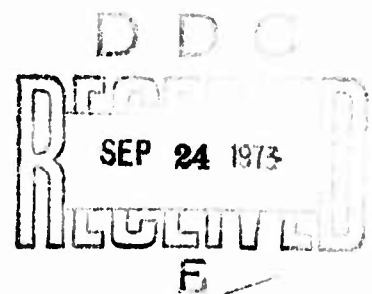
P. C. Fritsch  
R. E. Jordan

August 1973

Prepared for

DEPUTY FOR SURVEILLANCE AND CONTROL SYSTEMS

ELECTRONIC SYSTEMS DIVISION  
AIR FORCE SYSTEMS COMMAND  
UNITED STATES AIR FORCE  
L. G. Hanscom Field, Bedford, Massachusetts



Reproduced by  
NATIONAL TECHNICAL  
INFORMATION SERVICE  
U.S. Department of Commerce  
Springfield, VA. 22151

Approved for public release;  
distribution unlimited.

Project 4530

Prepared by  
THE MITRE CORPORATION  
Bedford, Massachusetts

Contract No. F19628-73-C-0001

## DOCUMENT CONTROL DATA - R &amp; D

(Security classification of title, body of abstract and indexing annotation must be entered when the overall report is classified)

1. ORIGINATING ACTIVITY (Corporate author) The MITRE Corporation P. O. Box 208 Bedford, Ma 01730		2a. REPORT SECURITY CLASSIFICATION UNCLASSIFIED	
		2b. GROUP	
3. REPORT TITLE Seek Storm Radar Sensitivity Study			
4. DESCRIPTIVE NOTES (Type of report and inclusive dates)			
5. AUTHOR(S) (First name, middle initial, last name) P. C. Fritsch R. E. Jordan			
6. REPORT DATE August 1973		7a. TOTAL NO. OF PAGES 79	7b. NO. OF REFS 9
8a. CONTRACT OR GRANT NO. F 19628-73-C-0001		9a. ORIGINATOR'S REPORT NUMBER(S) ESD-TR-73-134	
b. PROJECT NO. 4530		9b. OTHER REPORT NO(S) (Any other numbers that may be assigned this report) MTR-2487	
c.			
d.			
10. DISTRIBUTION STATEMENT Approved for public release; distribution unlimited.			
11. SUPPLEMENTARY NOTES		12. SPONSORING MILITARY ACTIVITY Deputy for Surveillance and Control Systems Electronic Systems Division, AFSC L. G. Hanscom Field, Bedford, Ma 01730	
13. ABSTRACT <p>This report describes the relationship between various radar parameters, earth geometrical parameters and hurricane rain rate parameters. An attempt is made to illustrate in graphical form the radar performance sensitivity to each parameter. These sensitivity results can be used as a design basis for a realistic radar system to observe and measure important characteristics of a hurricane weather occurrence.</p>			

14. KEY WORDS	LINK A		LINK B		LINK C	
	ROLE	WT	ROLE	WT	ROLE	WT
HURRICANE WEATHER						
RADAR DEVELOPMENT						
RADAR PARAMETERS						
RADAR PERFORMANCE SENSITIVITY						
STORM MAPPING						

SEEK STORM RADAR SENSITIVITY STUDY

P. C. Fritsch  
R. E. Jordan

August 1973

Prepared for

DEPUTY FOR SURVEILLANCE AND CONTROL SYSTEMS

ELECTRONIC SYSTEMS DIVISION  
AIR FORCE SYSTEMS COMMAND  
UNITED STATES AIR FORCE  
L. G. Hanscom Field, Bedford, Massachusetts



Approved for public release;  
distribution unlimited.

Project 4530

Prepared by

THE MITRE CORPORATION  
Bedford, Massachusetts

Contract No. F19628-73-C-0001


ib

## FOREWORD

The work described in this report was carried out under the sponsorship of the Deputy for Surveillance and Control Systems, Project 4530, by The MITRE Corporation, Bedford, Massachusetts, under Contract No. F19628-73-C-0001.

## REVIEW AND APPROVAL

Publication of this technical report does not constitute Air Force approval of the report's findings or conclusions. It is published only for the exchange and stimulation of ideas.

for 

H. J. McLOUD, JR., LT COL, USAF  
System Program Director  
Surveillance and Instrumentation SPO

## ABSTRACT

This report describes the relationship between various radar parameters, earth geometrical parameters and hurricane rain rate parameters. An attempt is made to illustrate in graphical form the radar performance sensitivity to each parameter. These sensitivity results can be used as a design basis for a realistic radar system to observe and measure important characteristics of a hurricane weather occurrence.

## PREFACE

This study has been performed on Project SEEK STORM to assist in defining radar parameter trade-offs which may be necessary prior to writing radar specifications. SEEK STORM is a radar development program which will eventually be incorporated into the Airborne Weather Reconnaissance System (AWRS). This radar must provide for cloud mapping of severe storms such as hurricanes so that rain intensity displays of the storm cells are available for weather prediction analysis. Of particular interest is the diameter of a hurricane eye, thickness of rain walls, rain intensity and overall height of the storm profile.

Operationally, there are further requirements for the radar to assist in navigation during aircraft penetration of severe storms and also to assist in navigation during severe weather conditions by providing a ground mapping capability. Since not all of these requirements can possibly be satisfied with a single radar, only the storm contour mapping function has been considered in this analysis. This function is considered the most important and perhaps the more difficult requirement to satisfy. As the radar design progresses, the capability of satisfying other requirements will be incorporated if this does not degrade the storm mapping capability. Otherwise, additional sensors will be required and defined later in the program.



## TABLE OF CONTENTS

	<u>Page</u>
LIST OF ILLUSTRATIONS	vii
LIST OF TABLES	viii
1.0 INTRODUCTION	1
2.0 METEOROLOGICAL RADAR EQUATION	2
2.1 Basic Radar Range Equation	2
2.2 Weather Radar Cross Section	2
2.3 Reflectivity	3
2.4 Receiver Bandwidth and Antenna Gain	4
2.5 Parameter Sensitivity versus Signal-to-Noise Ratio	5
2.6 Other Considerations	6
3.0 ANTENNA PATTERN BEAMWIDTHS	10
3.1 Vertical Antenna Beamwidth	12
3.1.1 Storm Height versus Radar Range	12
3.1.2 Signal-to-Clutter	15
3.2 Horizontal Antenna Beamwidth	44
3.2.1 Beamwidth versus Angular Resolution	44
3.2.2 Azimuth Scanning Rate versus Number of Pulses Sampled	56
3.3 RF Frequency	59
3.3.1 Attenuation	59
3.3.2 Antenna Size	67
3.3.3 Transmitter Peak Power	69
REFERENCES	73

## LIST OF ILLUSTRATIONS

<u>Figure Number</u>		<u>Page</u>
1.0	Range Resolution versus Pulse Width	8
2.0	Typical Antenna Pattern	11
3.0	Storm Height versus Range	13
4.0	Storm Height versus Range	14
5.0	Hurricane Storm Model	16
6.0	Aircraft Altitude versus Distance to Horizon	17
7.0	Signal to Clutter Geometry	19
8.0	Reflectivity versus Rain Rate	21
9.0	Rain Rate versus Reflectivity	22
10.0	Percent Power versus Normalized Angle from Boresight	25
11.0	BFF Geometry	27
12.0	Earth Geometry (Aircraft at 4.4K Ft.)	28
13.0	Elevation Look Angle and Altitude versus Range (A/C at 10K Ft.)	29
14.0	Earth Geometry-Aircraft at 22K Ft.	30
15.0	Storm Height Geometry	32
16.0	Rain Rate Error Factor versus BFF (for Non-Attenuating Wavelengths)	34
17.0	Signal to Clutter Geometry	37
18.0	BIF <sub>1</sub> versus Normalized Beam Angles	39
19.0	BIF <sub>2</sub> versus Normalized $\theta$	40
20.0	Beam Depression Factor versus Normalized Depression Angle	41
21.0	Signal to Clutter versus Elevation Look Angle	45
22.0	Beam Position Relative to Hurricane Eye	47
23.0	Relative Power versus Beam Position	49
24.0	Relative Power versus Scan Angle	50
25.0	Relative Power versus Normalized Horizontal Beamwidth	51
26.0	Range versus $\epsilon$	52
27.0	Radar-Rain Cell Geometry	54
28.0	Azimuth Distortion of Rain Cells	55
29.0	Attenuation versus Frequency	60
30.0	Antenna Characteristics	61
31.0	Attenuation Loss Due to Rain Over 100 km Path Length	63
32.0	Total Path Attenuation and Half Power Beamwidth versus Frequency	64
33.0	Affect of BFF on Rain Rate Estimate	66

## LIST OF TABLES

<u>Table Number</u>		<u>Page</u>
I	Example of Beam Filling Factors	31
II	Signal to Clutter versus Beamwidth and Frequency	42
III	Antenna Parameters	68
IV	Peak Power Variations	70
V	Peak Power Variations	71

## 1.0 INTRODUCTION

This sensitivity analysis has been performed to determine sensitivity of the various radar parameters (such as, antenna gain, beamwidths, power transmitted, frequency, pulse width, pulse repetition frequency, etc.) to performance of the SEEK STORM radar. Effects of each parameter on the radar signal output will indicate the extent to which each parameter can be varied without degrading required performance. Results of this analysis will be used to initiate a three-dimensional computer simulation consisting of a storm model, an airborne radar and earth geometry. Radar parameter selection for this simulation will be obtained from the results of this analysis.

## 2.0 METEOROLOGICAL RADAR EQUATION

### 2.1 Basic Radar Range Equation

Signal to noise ratio ( $\frac{S}{N}$ ) received by a radar can be determined by the equation <sup>(1)</sup>

$$\frac{S}{N} = \frac{P_T G^2 \lambda^2 \sigma}{(4\pi)^3 R^4 k T B \overline{NF} L} \quad (1)$$

where;

$P_T$  = peak transmitted power

$G$  = antenna gain

$\lambda$  = wavelength of the RF frequency transmission

$\sigma$  = target radar cross section

$R$  = range to target

$k$  = Boltzmann's constant

$T$  = standard temperature 290°K

$B$  = receiver bandwidth

$L$  = round trip attenuation through propagating medium

$\overline{NF}$  = receiver noise figure.

### 2.2 Weather Radar Cross Section

For extended targets such as rain clouds, the radar cross section (assuming the rain fully fills the beam) can be expressed as the product of radar resolution volume ( $V_m$ ) and the average back-scatter cross section of particles per unit volume ( $\sum_i \sigma_i$ )

$$\sigma = V_m \sum_i \sigma_i \quad (2)$$

Radar resolution volume can be approximated in terms of azimuth beamwidth ( $\theta_A$ ), elevation beamwidth ( $\theta_E$ ), radar range (R) and the range increment corresponding to the two-way travel time of the radar pulse length ( $\tau$ ) as:

$$V_m = \frac{\pi}{4} R^2 \theta_A \theta_E \frac{c\tau}{2}, \quad (3)$$

where  $c$  is the velocity of propagation of the radar signal.

By assuming Rayleigh scattering (where the wavelength is long compared to particle size) the radar cross section of each rain particle of diameter (D) can be written as:

$$\sigma_i = \frac{\pi^5 D^6}{\lambda^4} |K|^2, \quad (4)$$

where  $K$  is a constant dependent upon the dielectric constant of the scatterers. For water at  $10^\circ\text{C}$  the value of  $|K|^2$  is 0.93.

### 2.3 Reflectivity

Reflectivity factor (Z) is defined as the sum of the sixth power of the raindrop diameters in a unit volume and may be written as:

$$Z = \sum_i D^6 \quad (5)$$

Reflectivity can also be expressed as  $Z = a \overline{RR}^b$  where  $a$  and  $b$

are empirical constants and  $\overline{RR}$  is the rain rate in millimeters per hour. By substituting Equations (2), (3), (4), and (5) into Equation (1), we obtain:

$$\frac{S}{N} = \frac{P_T G^2 \pi^3 Z |K|^2 \theta_A \theta_E c \tau}{(8)^3 R^2 \lambda^2 k T B \overline{NF} L} \quad (6)$$

#### 2.4 Receiver Bandwidth and Antenna Gain

For a receiver which is matched to the transmitted pulse, the bandwidth can be approximated as:

$$B \approx \frac{2}{\tau} \quad (7)$$

Antenna gain  $G$  can also be expressed in terms of aperture area as<sup>(2)</sup> 1

$$G = \frac{4 \pi W H}{\lambda^2} N = \frac{4 \pi}{\theta_A \theta_E} N \quad (8)$$

where (assuming a rectangular aperture);

$W$  = antenna width

$H$  = antenna height

$N$  = antenna aperture efficiency factor.

---

<sup>1</sup> $N$  has been replaced for  $\eta$  in the reference because  $\eta$  is used for another purpose in this report.

## 2.5 Parameter Sensitivity versus Signal-to-Noise Ratio

Equations (7) and (8) can be combined with Equation (6) to obtain:

$$\frac{S}{N} = \bar{K} \frac{P_T \tau^2 Z}{R^2 \lambda^2 \theta_A \theta_E L} \quad (9)$$

where;

$$\bar{K} = \frac{\pi^5 N^2 |K|^2 c}{(8)^2 k T \overline{NF}}$$

If  $\theta_A \theta_E$  were substituted by  $\frac{4\pi}{G}$  in Equation (9) as indicated by Equation (8) it can be seen that the S/N is proportional to G and not  $G^2$  as is normally the case with the point targets. This means that a weather radar is not as dependent upon antenna gain as the usual target detection radar. Note also that the weather radar S/N sensitivity to range is proportional to  $\frac{1}{R^2}$  whereas the a point target S/N is proportional to  $\frac{1}{R^4}$ . If signal-to-noise were the only criterion to use in this radar design, one can readily see from Equation (9) the effect of each parameter on the radar output. To obtain a high signal-to-noise level, all parameters in the numerator should be made as large as possible and all parameters in the denominator should be made as small as possible. Parameters which have exponents (such as  $\lambda^2$  and  $\tau^2$ ) affect the signal-to-noise level much more than those which do not have exponents. The problem of selecting small values in the denominator to represent wavelength



and antenna beamwidths is subject to many theoretical and practical considerations which must be investigated.

## 2.6 Other Considerations

As stated, the SEEK STORM radar has both practical and theoretical requirements which are not directly considered in the radar range equation. The main practical consideration is the antenna size. This radar is to be mounted on a C130 aircraft and therefore the maximum antenna size will be constrained by the aircraft aerodynamics and structures. This study will therefore attempt to determine the minimum size antenna which can be used.

Radar resolution requirements are determined by pulsewidth ( $\tau$ ) and antenna beamwidths  $\theta_A$  and  $\theta_E$ . The beamwidths for a given aperture ( $W \times H$ ) are a function of wavelength (as implied in Equation 8) which in turn is determined by frequency selected.

Equation (9) does take into consideration attenuation effects ( $L$ ) of the two-way transmission of electromagnetic energy as it propagates in and out of the storm cells. Attenuation in decibels is inversely proportional to approximately the fourth power of wavelength. That is, as wavelength increases, attenuation decreases very rapidly. However, as wavelength increases, antenna size required to obtain desired beamwidths necessary for good resolution also increases. An increase in vertical beamwidth, in particular, will cause an increase in ground or sea clutter return because more transmitted energy is likely to be intercepted by the earth surface. Therefore, we not only must consider signal-to-noise levels but also signal-to-clutter levels. Thus we can see that frequency and wavelength selection along with beamwidths and antenna size are all

interrelated by both theoretical and practical requirements. Once these parameters are determined, the transmitted peak power ( $P_T$ ) can be adjusted to obtain an optimum received signal level. Available airborne average power ( $P_{AVG}$ ) must also be taken into consideration along with pulse repetition frequency (PRF) and pulsewidth ( $\tau$ ) after the peak power requirements are determined since:

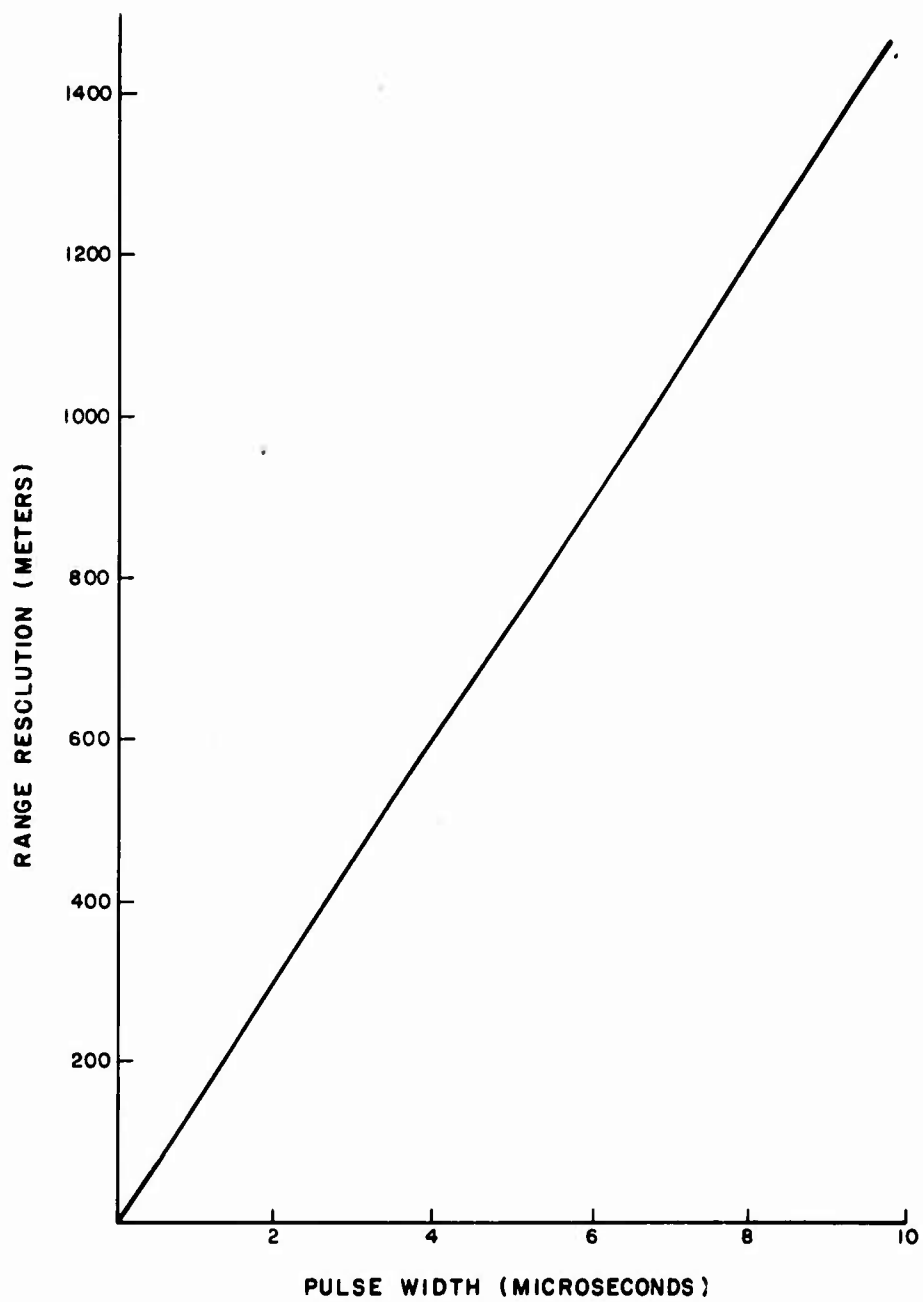
$$P_T = \frac{P_{AVG}}{\tau (PRF)} \quad (10)$$

The pulsewidth is dictated by range resolution requirements since the range resolution of extended targets is equal to  $\frac{c\tau}{2}$ . Figure 1.0 illustrates range resolution versus pulsewidth.

Maximum pulse repetition frequency is determined by the maximum range of interest to the radar. In the SEEK STORM radar this maximum range of interest is about 250 nautical miles. Since the round trip travel time of a pulse is approximately 12 microseconds per nautical mile; a time interval of 3000 microseconds must be present between succeeding pulses. This means that the PRF should be no greater than 300 pulses per second.

Both the rain return signal and the receiver noise have wide fluctuations about their mean (average value). Their sum also fluctuates widely. In mathematical terms, the variance of the probability density function of S, N, and (S+N) is large for single samples (single pulse basis). This could result in large errors in estimating rain reflectivity, even if  $S/N \rightarrow \infty$ .

When, however, many independent pulse samples are averaged, the variance decreases progressively as the number of samples increases. Under these conditions one can still obtain good estimates of rain reflectivity for relatively low S/N ratios.



18-38,253

Figure 1.0 RANGE RESOLUTION VERSUS PULSE WIDTH

This can be performed in the following manner: Assuming a finite ratio  $S/N$ , integrating many statistically independent samples will result in a good estimate of  $(S+N)$ . By instrumenting the radar to provide a continuously updated value for  $N$ , an accurate estimate of  $S$  can now be made by subtraction. This value of  $S$  is directly proportional to the average radar rain reflectivity factor  $Z$ .

### 3.0 ANTENNA PATTERN BEAMWIDTHS

As seen from the previous section, performance of the SEEK STORM mapping radar depends heavily upon the characteristics of the antenna system. The vertical beamwidth of the antenna pattern for a certain wavelength is dependent upon the height of the antenna and the horizontal beamwidth is dependent upon the width of the antenna. As these sizes increase, the corresponding beamwidths decrease. To determine beamwidth in the vertical or elevation plane, the height of storms, altitude of the aircraft and influence of ground clutter must be considered. To determine beamwidth in the horizontal or azimuthal plane, angular resolution of storm cells must be considered. The accuracy to which the radar is able to predict rain intensity at a given point in an actual storm is also a function of both the azimuth and elevation beamwidth. To study these effects, it is convenient to select a typical antenna pattern which is well within present practical design capabilities.

The prototype antenna pattern which will be used in this study for both the vertical and horizontal directions is the far field pattern of a circular or elliptical antenna aperture illuminated by a particular "cosine-on-a-pedestal feed pattern."<sup>(3)2</sup> This corresponds to typical "dish" antenna design practice, although implementation by a slot array, such as the "flat-plate" type of antenna, is possible. Figure 2.0 is a graphical representation of this antenna

---

<sup>2</sup>The selected illumination function,  $0.2 + 0.8 \cos \pi x$ , causes an edge illumination of approximately -14 dB. While details of patterns due to other illumination functions may differ somewhat, it is felt that this particular pattern is representative of a wide class of commonly encountered antenna patterns.

IA-38,228

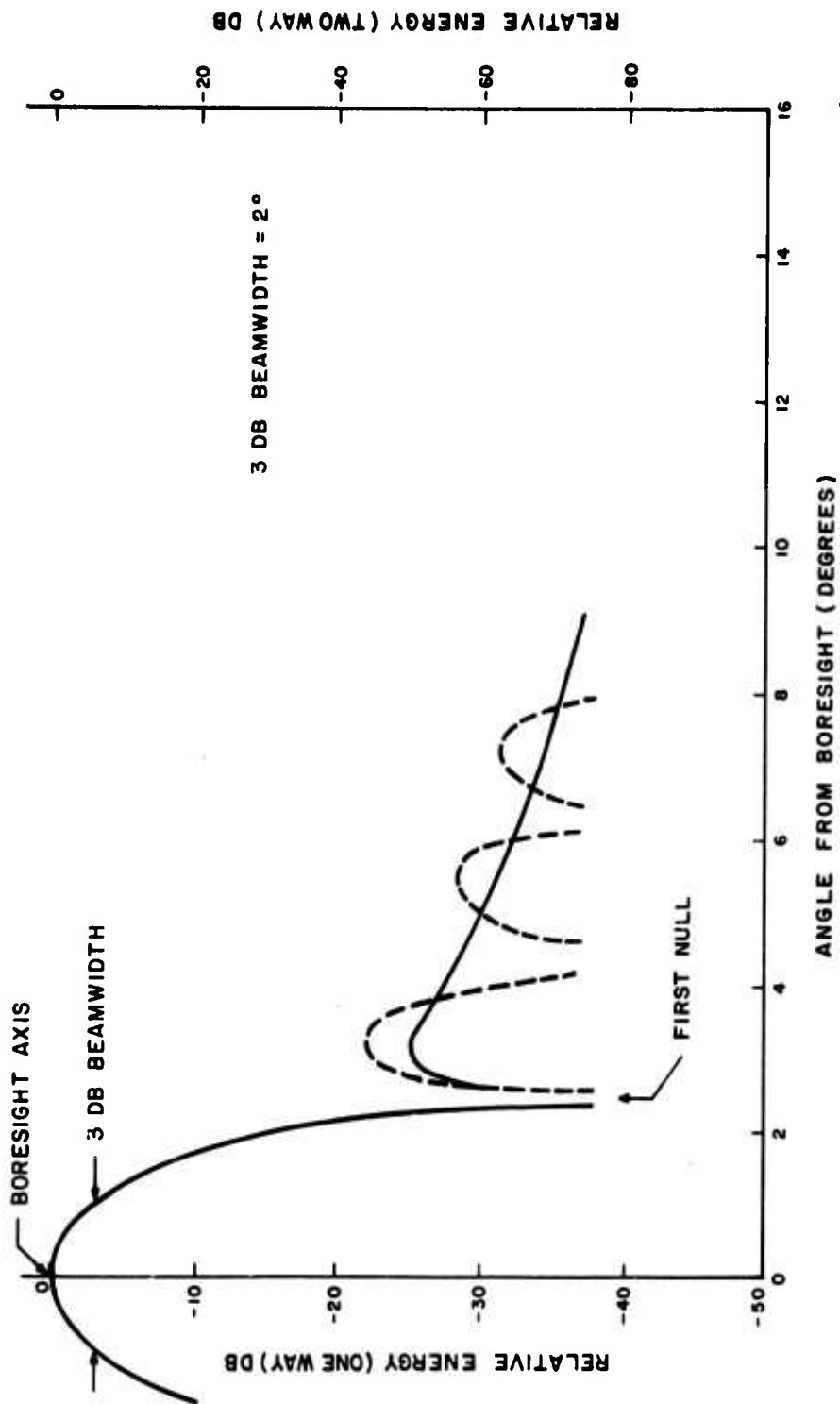


Figure 2.0 TYPICAL ANTENNA PATTERN

pattern with an indicated 3 dB beamwidth of  $2.0^{\circ}$ . Within limits which are not exceeded in this study, patterns of other beamwidths can be scaled from this graph. The actual sidelobes (dashed) have been replaced for convenience by an approximate average level (solid line). The one-way pattern can conveniently be converted to a two-way pattern by multiplying the ordinates, in decibels, by a factor of two (as at the right hand margin of Figure 2.0).

In studying Figure 2.0, particular attention should be paid to the first null (shown at  $\sim 2.5^{\circ}$ ). Note how rapidly the antenna sensitivity changes in this region: the two-way pattern, for instance, changes 40 dB in a  $0.2^{\circ}$  increment near the null. This corresponds to a rate of change of sensitivity in that region of 200 dB/degree. Also noteworthy is the peak of the first sidelobe which is about 22 dB below the main lobe on the one-way pattern and 44 dB below the main lobe on the two-way pattern. The importance of these factors will become apparent in later discussions. This pattern will first be used to analyze the system sensitivity to vertical antenna beamwidth.

### 3.1 Vertical Antenna Beamwidth

#### 3.1.1 Storm Height versus Radar Range

To consider geometry of the situation, a  $4/3$  earth curvature has been assumed to compensate for atmospheric refraction of electromagnetic energy. Figures 3.0 and 4.0 illustrate how the earth curvature affects radar range versus storm height for an aircraft at 10,000 and 22,000 feet altitude using various elevation look angles. The elevation look angle is defined here as the angle measured from the aircraft line of sight to the radar horizon.

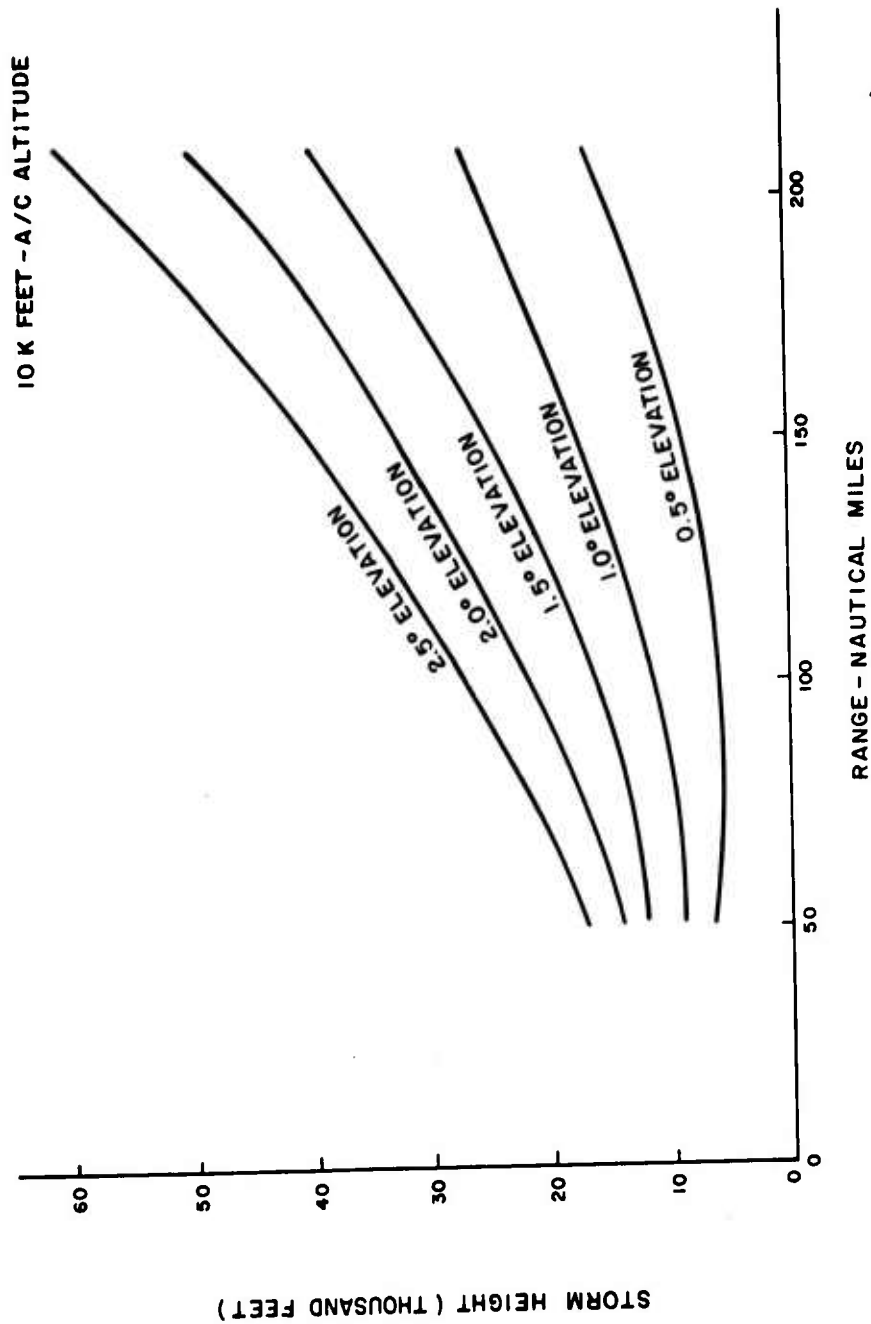


Figure 3.0 STORM HEIGHT VERSUS RANGE

1A-38,224



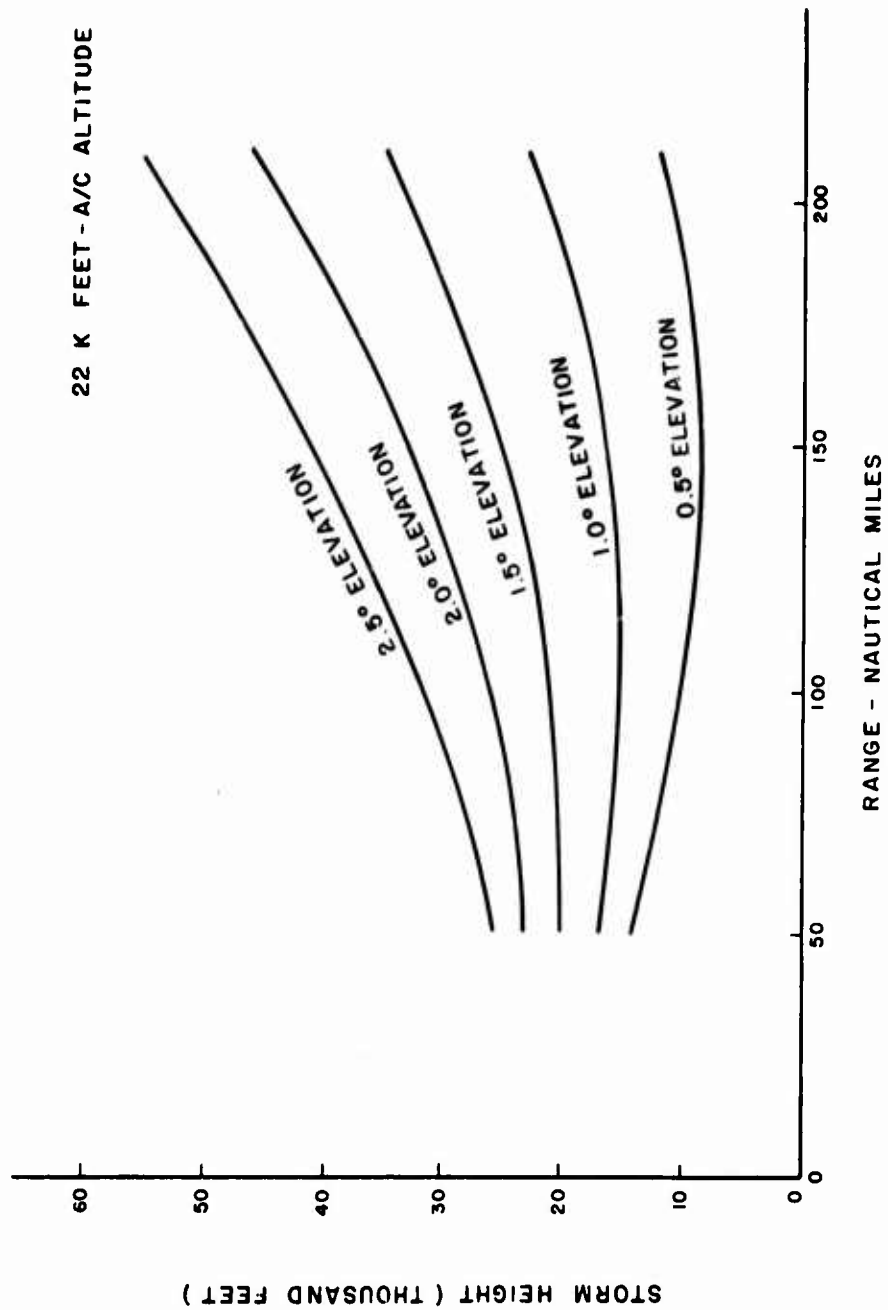


Figure 4.0 STORM HEIGHT VERSUS RANGE

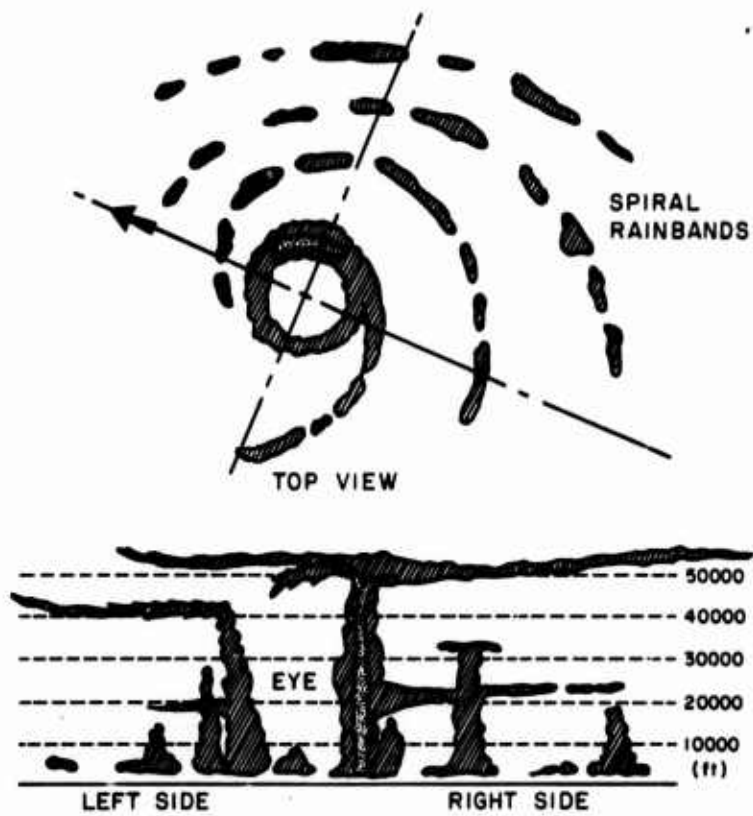
A hurricane model profile (shown in Figure 5.0) developed from years of experience by the National Hurricane Research Laboratory indicates storm height could be as high as 50,000 feet. To show how these curves can be used, suppose the aircraft altitude were 10,000 feet (Figure 3.0) and the top of the vertical beam pattern was at an elevation look angle of 1.5 degrees, then a point in the storm at 30,000 feet altitude could be seen out to a range of 175 nautical miles. If the aircraft were higher at say an altitude of 22,000 feet (Figure 4.0) then the same point could be seen at a range of 183 nautical miles for the same elevation look angle of 1.5 degrees. The increase in aircraft altitude does not gain a very appreciable range advantage. However, these curves do indicate how the line of sight radar range varies with storm height if the entire vertical beamwidth is to be uniformly filled with the storm.

If only one half of the beam were to intercept the storm, then an error in measuring the reflectivity factor of approximately 3 dB would occur because with no apriori knowledge, the radar must assume 100% beam filling. While the highest part of the vertical beam pattern should subtend storm heights for good measurement accuracy of reflectivity, the lowest portion of the pattern is likely to intercept the ground if the total vertical beamwidth is too wide. It is therefore, necessary to consider how sea clutter affects system performance at ranges less than the radar horizon and how earth shadowing affects performance at ranges greater than the radar horizon.

### 3.1.2 Signal-to-Clutter

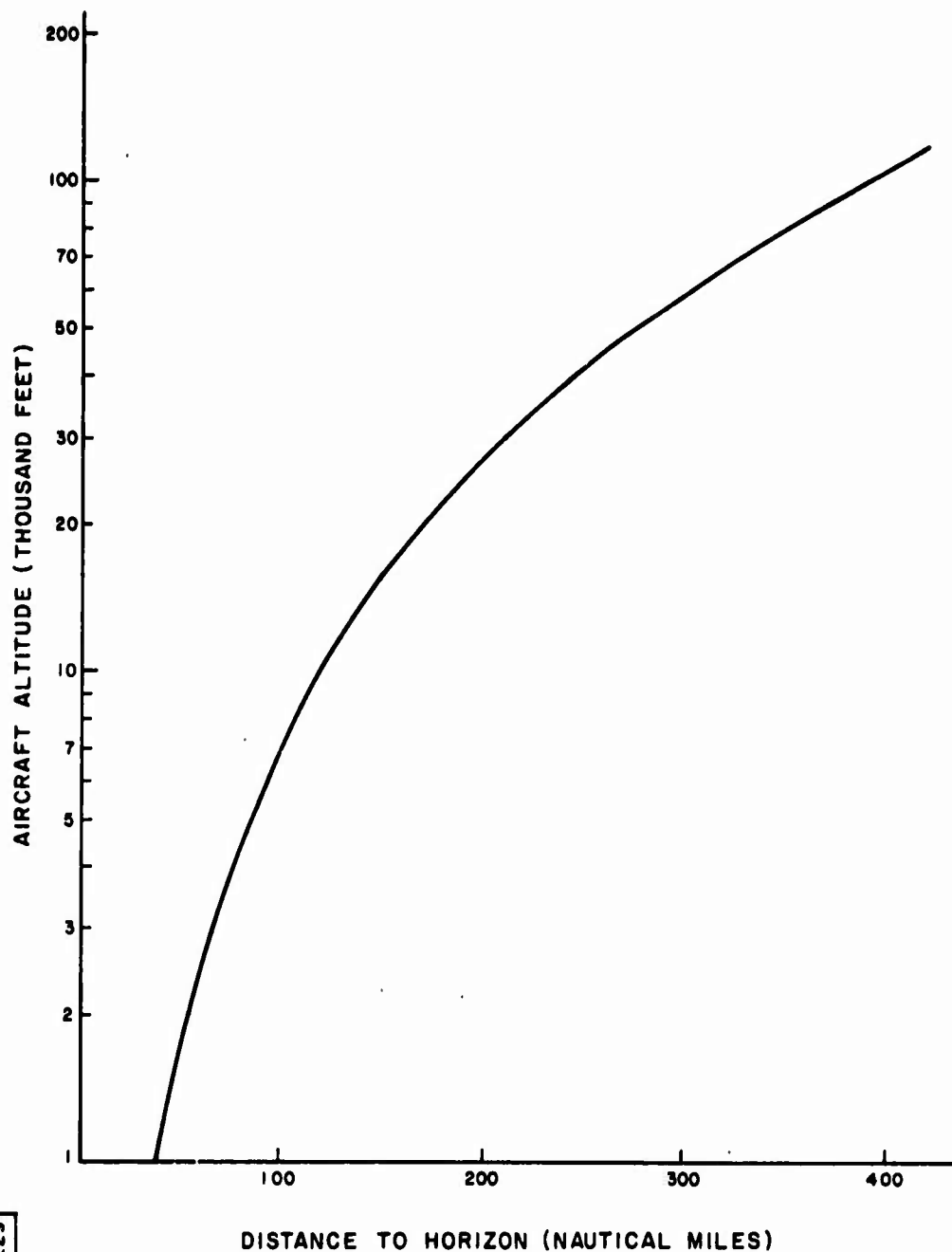
#### 3.1.2.1 Beam Fill Factor

At all radar ranges up to the radar horizon distance (see Figure 6.0) power radiated by the antenna toward the surface of the



IA - 38,225

Figure 5.0 HURRICANE STORM MODEL



IA-36,229

Figure 6.0 AIRCRAFT ALTITUDE VERSUS DISTANCE TO HORIZON

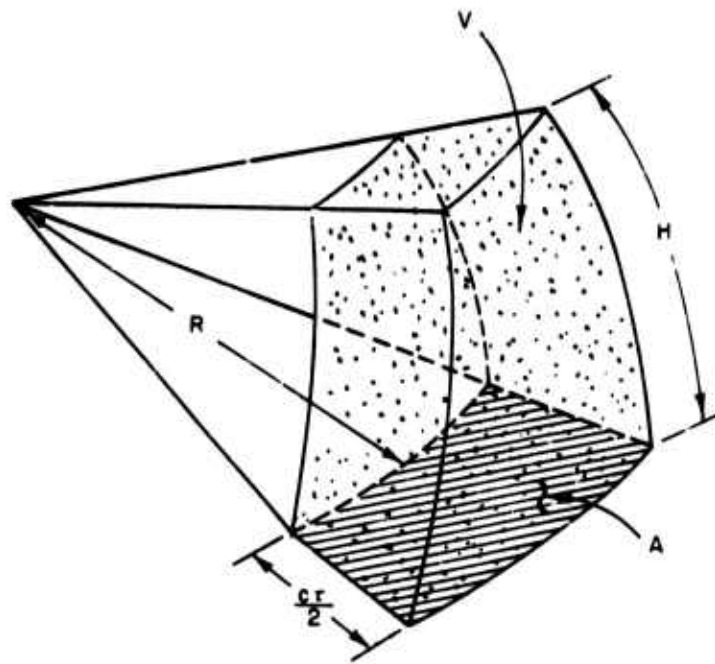
ground or sea below is partially scattered back toward the radar. If sufficiently large, this clutter return will interfere with the identification and measurement of the signal returned by the storm since the radar is unable to discriminate between two targets lying in the same range cell. For the SEEK STORM radar, all clutter return will be assumed to be sea clutter since this system is primarily being designed to obtain data on hurricanes before they reach land.

The geometry of these two competing targets is diagrammed in Figure 7.0 which approximates the radar volume to be rectangular instead of elliptical. The sea return is due to backscatter from area A. This is approximately a rectangle whose length (parallel to the range direction) is  $\frac{cT}{2}$ , the range resolution cell size. Its width is  $R \cdot \theta_A$ , where R is the radar range and  $\theta_A$  is the effective azimuth beamwidth. The total radar cross section due to area A is  $\sigma_{\text{sea}} = \sigma^0 A$ ;  $\sigma^0$  is the radar cross section per unit geometrical area<sup>3</sup> According to the most recent studies<sup>(4)</sup>, the value of  $\sigma^0$  is -40 dB for the present problem. This number is correct for horizontally polarized transmission and reception, frequencies between S and C band, and a fully developed sea under hurricane conditions (sea state #7).

The storm radar signal return is assumed to be due to backscatter from rain uniformly distributed throughout a volume V. The latter is approximately a rectangular prism of base area A. Its height is  $h = R \cdot \theta_E$ , where  $\theta_E$  is the effective antenna elevation beamwidth.

---

<sup>3</sup> $\sigma^0$  is pronounced "sigma super zero," since the "o" is a superscript (not an exponent).



IA-38,226

Figure 7 SIGNAL TO CLUTTER GEOMETRY

The radar cross section of the rain is then  $\sigma_{\text{rain}} = \eta \cdot V$ , where  $\eta$  is the radar cross section per unit volume, called radar reflectivity. The relationship between rainfall rates (RR) and  $\eta$  are shown in Figure 8.0 for various frequencies. These curves were computed from the empirical equations:

$$Z = 289 \text{ RR}^{1.4} \quad (11)$$

$$\eta = \frac{\pi^5 |K|^2}{\lambda^4} Z \quad (12)$$

Equation (11) is an empirical formula which was obtained from the National Hurricane Research Laboratory and is a result of statistical studies performed by that facility on hurricane storms. Figure 9.0 illustrates the relationship between Z and RR as indicated by Equation (11).

If area A and volume V are illuminated with equal radar power density, the power returned will be a function of the summation of the two radar cross sections since A and V are at the same radar range. Inasmuch as it is the rain which is of primary interest, its return is identified as "signal" (S). The sea return, being unwanted, is identified as "clutter" (C). The ratio of the two returns is thus the "signal-to-clutter ratio" ( $\frac{S}{C}$ ) which can be written as:

$$\frac{S}{C} = \frac{\sigma_{\text{rain}}}{\sigma_{\text{sea}}} = \frac{\eta \cdot V}{\sigma_o A} \quad (13)$$

---

<sup>4</sup>These equations assume a hypothetical situation where all of the beam volume is filled with rain and the beam is hitting the ground at a point where equal radar power density is illuminating both the rain and the ground.

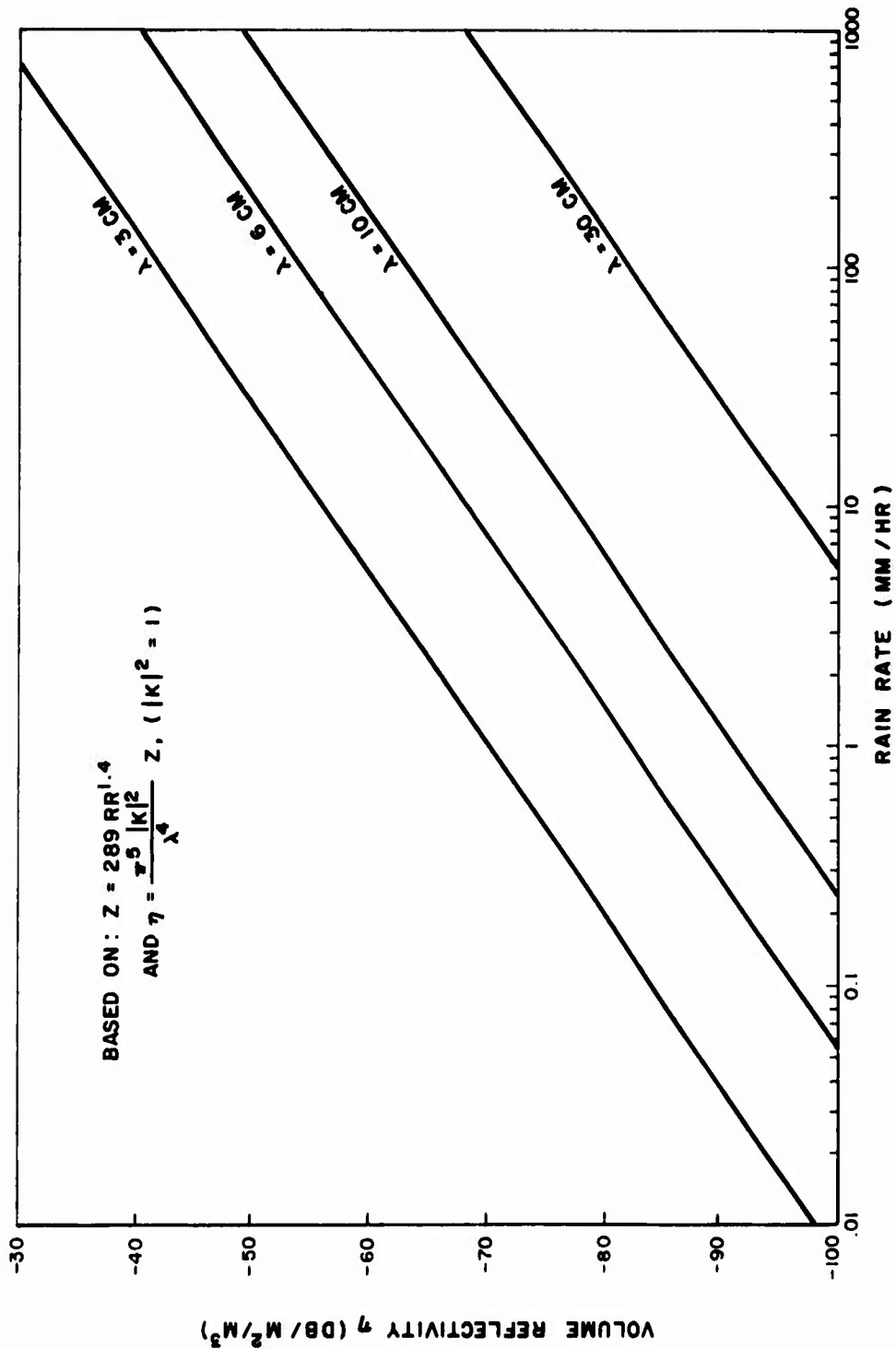


Figure 8.0 REFLECTIVITY VERSUS RAIN RATE



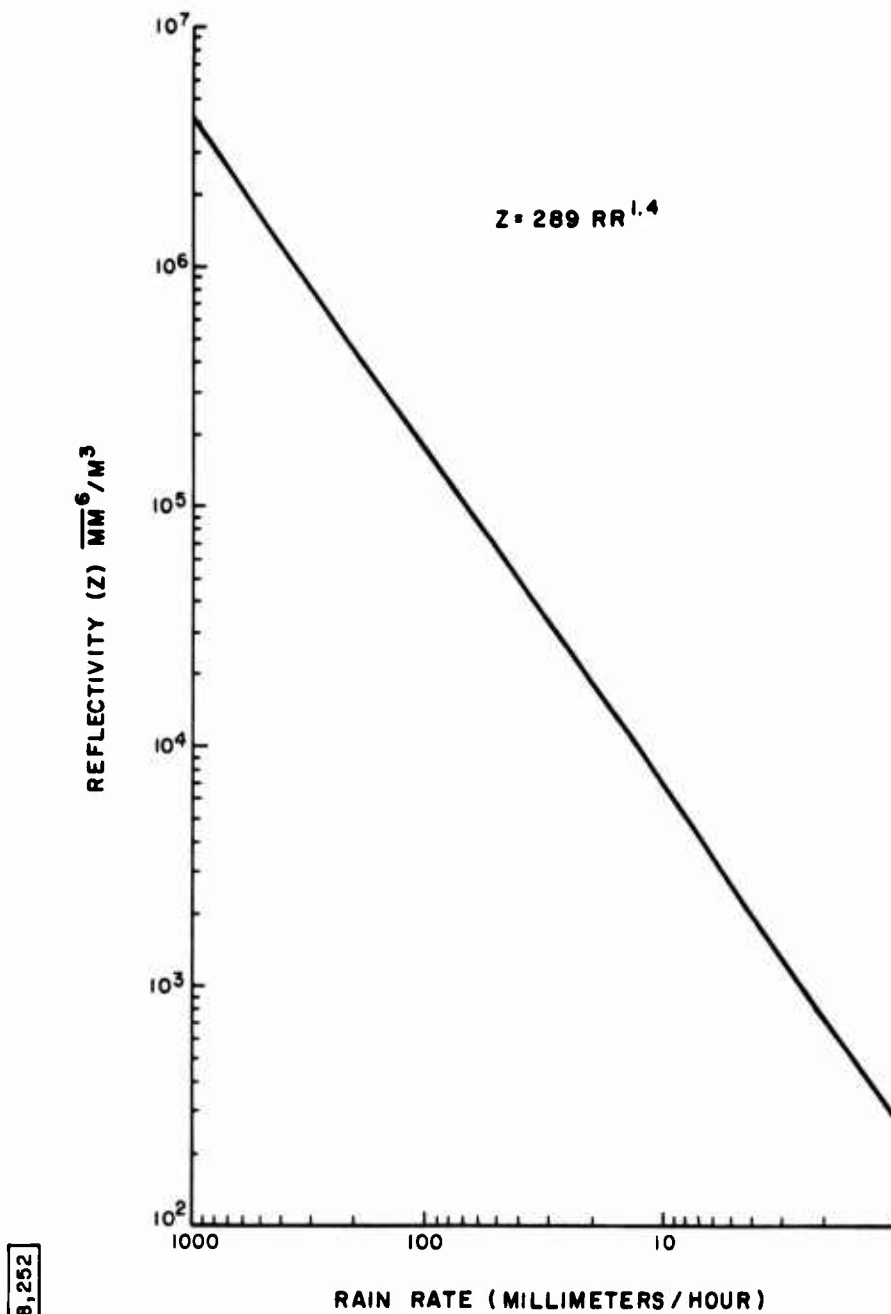


Figure 9.0 RAIN RATE VERSUS REFLECTIVITY

The rain volume  $V$  is approximately  $\frac{c\tau}{2} (R\theta_A) (R\theta_E)$ . The sea area  $A$  is  $\frac{c\tau}{2} R\theta_A$ . Equation (11) can now be written as:

$$\frac{S}{C} = \eta \frac{R\theta_E^5}{\sigma^0} \quad (14)$$

Note that this equation shows signal-to-clutter to be completely independent of azimuth beamwidth and pulse length. Since the parameters  $\eta$ ,  $R$  and  $\sigma^0$  are uncontrolled variables, the signal-to-clutter sensitivity becomes dependent upon selection of elevation beamwidth. This neglects elevation pointing of the antenna which naturally also affects S/C ratio. If in Equation (13) the area  $A$  is zero, then signal-to-clutter is no problem because the S/C ratio would be infinite. This suggests that perhaps the beam should be kept up (off the ground). Figures 3 and 4 show the extent of the elevation angle on the highest part of the vertical beam due to storm heights of interest if all of the vertical beamwidth is to subtend the clouds. We must now determine how much of the beam can illuminate the ground or sea and still maintain a reasonable S/C ratio. A 10 dB to 20 dB  $\frac{S}{C}$  ratio is considered reasonable for this application. In areas of no rain (such as between rain bands) a different clutter criterion must be used. In this region, the radar will interpret the sea clutter return as rain. This will result in two basic sources of error. The first is simply an indication of rain in a no rain area. The second error occurs when rain attenuation must be taken into account. The erroneous rain indication could result in an excessive attenuation estimate causing large error in rain prediction.

---

<sup>5</sup> These equations assume a hypothetical situation where all of the beam volume is filled with rain and the beam is hitting the ground at a point where equal radar power density is illuminating both the rain and the ground.

If the center of a beam is pointed at a fixed elevation and the (boresight) beamwidth is allowed to increase, then at distances less than the horizon (Figure 6.0) some portion of the beam is eventually intercepted by the earth surface. This means that not all of the  $R\theta_E$  distance (Equation 14) is being subtended by storm rain clouds and therefore not all of the antenna beamwidth is contributing to signal return from rain alone. The portion of the beam which intercepts the ground will add sea clutter return. Also when the top part of the beam is higher than the storm rain clouds, the upper portion of the arc length  $R\theta_E$  is not contributing to signal return. Furthermore, under these conditions the rain and sea surface are not being irradiated at equal power density. To take these factors into consideration we must introduce a "beam fill factor" (BFF).

The BFF is defined as the ratio of beam power intercepted by the rain to the total effective beam power on a two-way basis.

To determine the BFF it is necessary to relate a typical antenna beam pattern such as is shown in Figure 2 to the percentage of power due to an incremental increase of angle from boresight which is transmitted in that beam pattern. This energy relationship to angle from boresight has been calculated and is illustrated in Figure 10. The dotted curve indicates the beam pattern which is included for

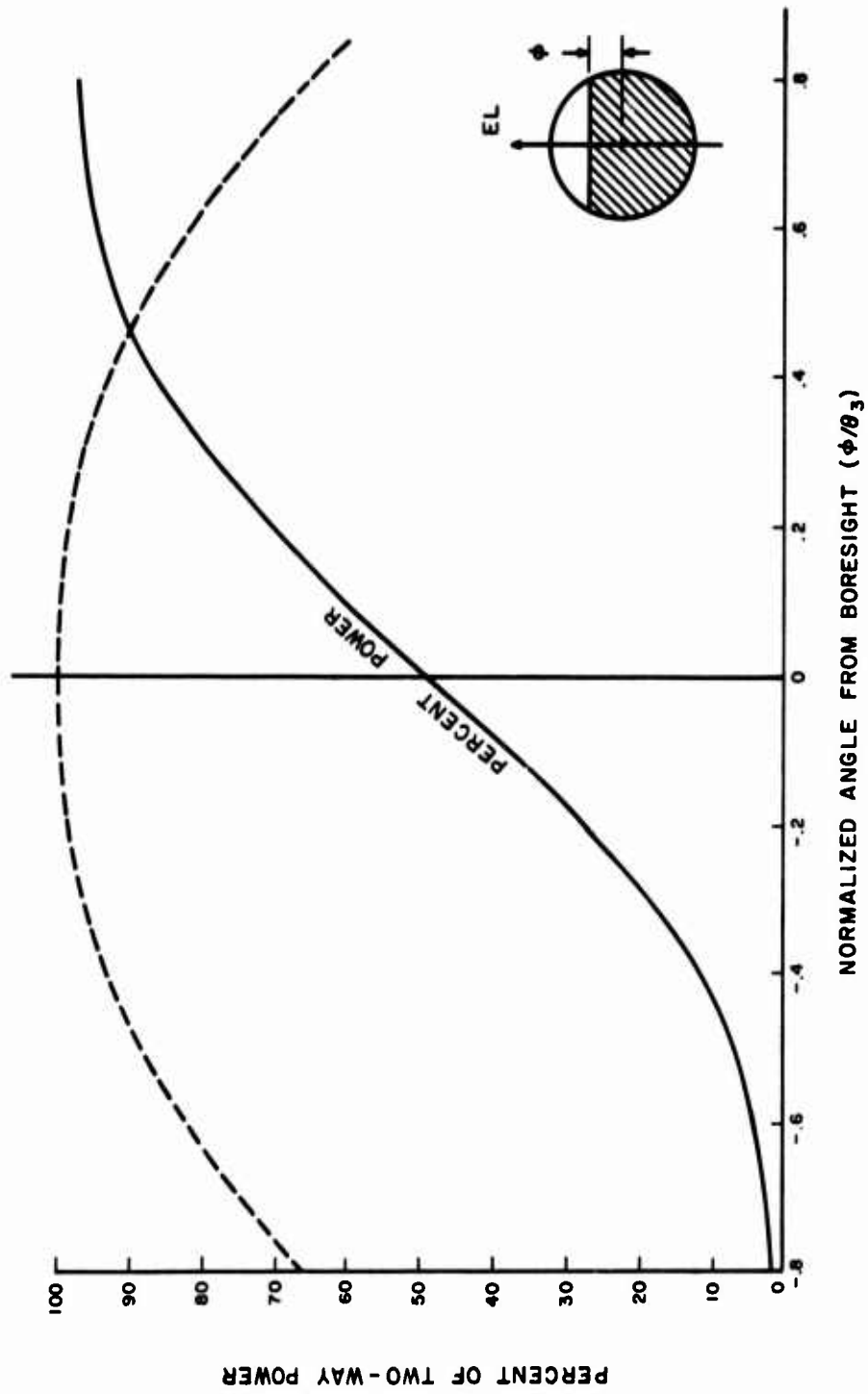


Figure 10.0 PERCENT POWER VERSUS NORMALIZED ANGLE FROM BORESIGHT

orientation purposes only. The abscissa is a normalized scale of angle from boresight.  $\theta_3$  is any 3 dB beamwidth of interest and  $\emptyset$  is the angle from boresight. The angle  $\emptyset$  is designated  $\emptyset^+$  to represent the angle from boresight to the top of the storm.  $\emptyset^-$  is used to designate the angle from boresight to the earth tangent for weather beyond the radar horizon and from boresight to the sea surface (at the range of interest) for weather nearer than the radar horizon.

To illustrate how this curve is used, (refer to Figure 11.0) suppose the vertical beam pattern is 3 degrees wide at the 3 dB points of the one-way pattern ( $\theta_3 = 3^\circ$ ). Assume that the boresight axis is pointed such that the top of the rain clouds are 1/2 degree above the boresight at the range of interest and that the angle from boresight to the earth surface which is shading some of the lower part of the beam is 1 degree. For this case  $\emptyset^+ = +0.5^\circ$  and  $\emptyset^- = 1.0^\circ$ . These two values of  $\emptyset$  are first normalized to the 3 dB beamwidth ( $\frac{0.5}{3} = +.166$  and  $\frac{1.0}{3} = -.333$ ). The value of  $+.166$  corresponds to the 70% power value in Figure 10. This means that 70% of the two-way power exists between the extreme bottom of the beam and the top of the rain clouds. To take the earth shadowed area into consideration, the  $-.333$  point corresponds to 17% of the two-way power. The percentage of beam energy which is intercepted by the rain cloud is therefore 53% ( $70 - 17 = 53$ ). The value of BFF in this case would be 0.53%.

To determine angular intercept points for various vertical beamwidths at different aircraft altitudes and at different boresight look angles it is convenient to use charts as shown in Figures 12, 13, and 14. These charts show the vertical profile of earth geometry for aircraft at 4400, 10,000 and 22,000 feet. The elevation look angles with respect to the radar horizon tangent for each aircraft altitude are also shown.

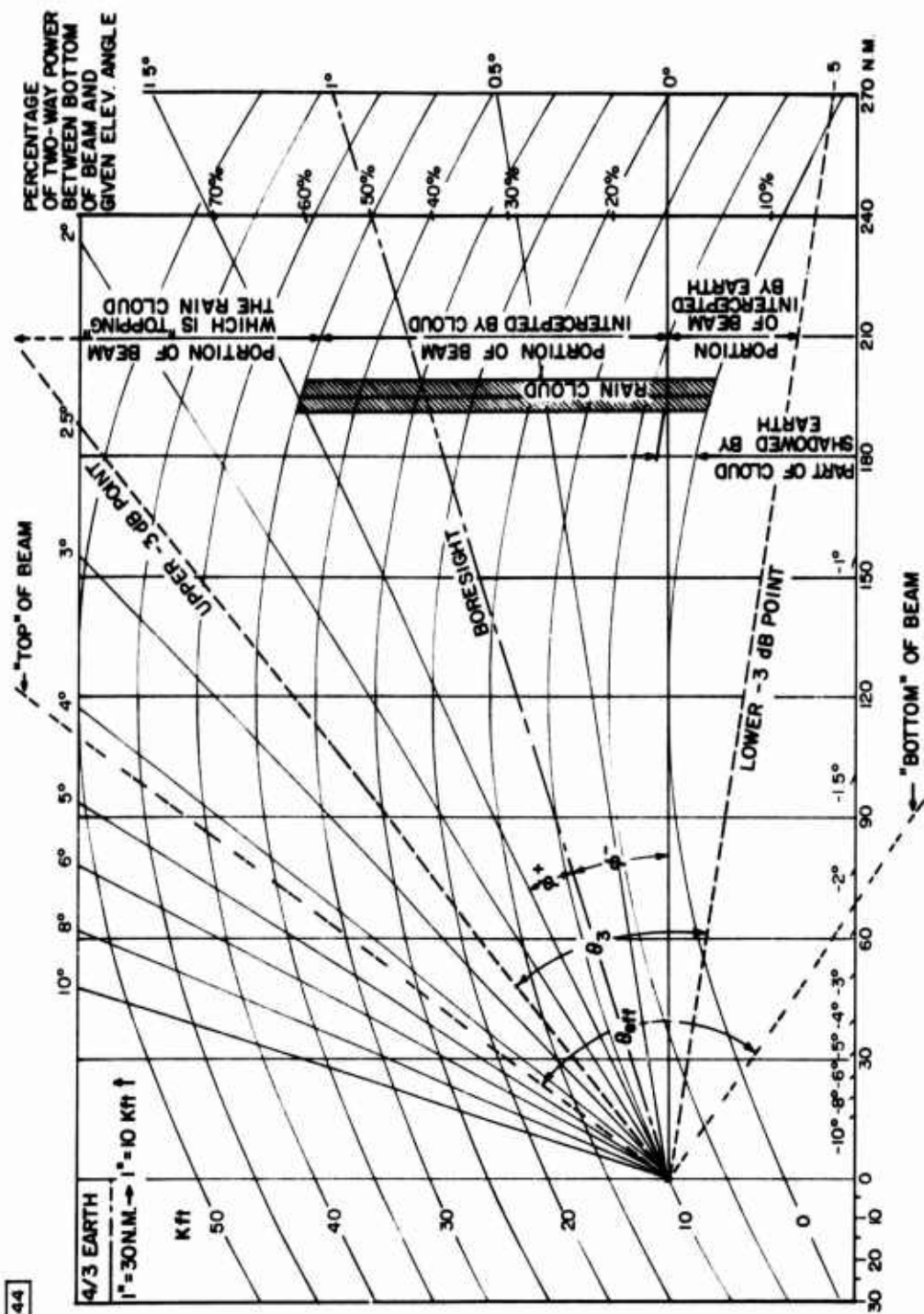


Figure 11.0 BFF GEOMETRY

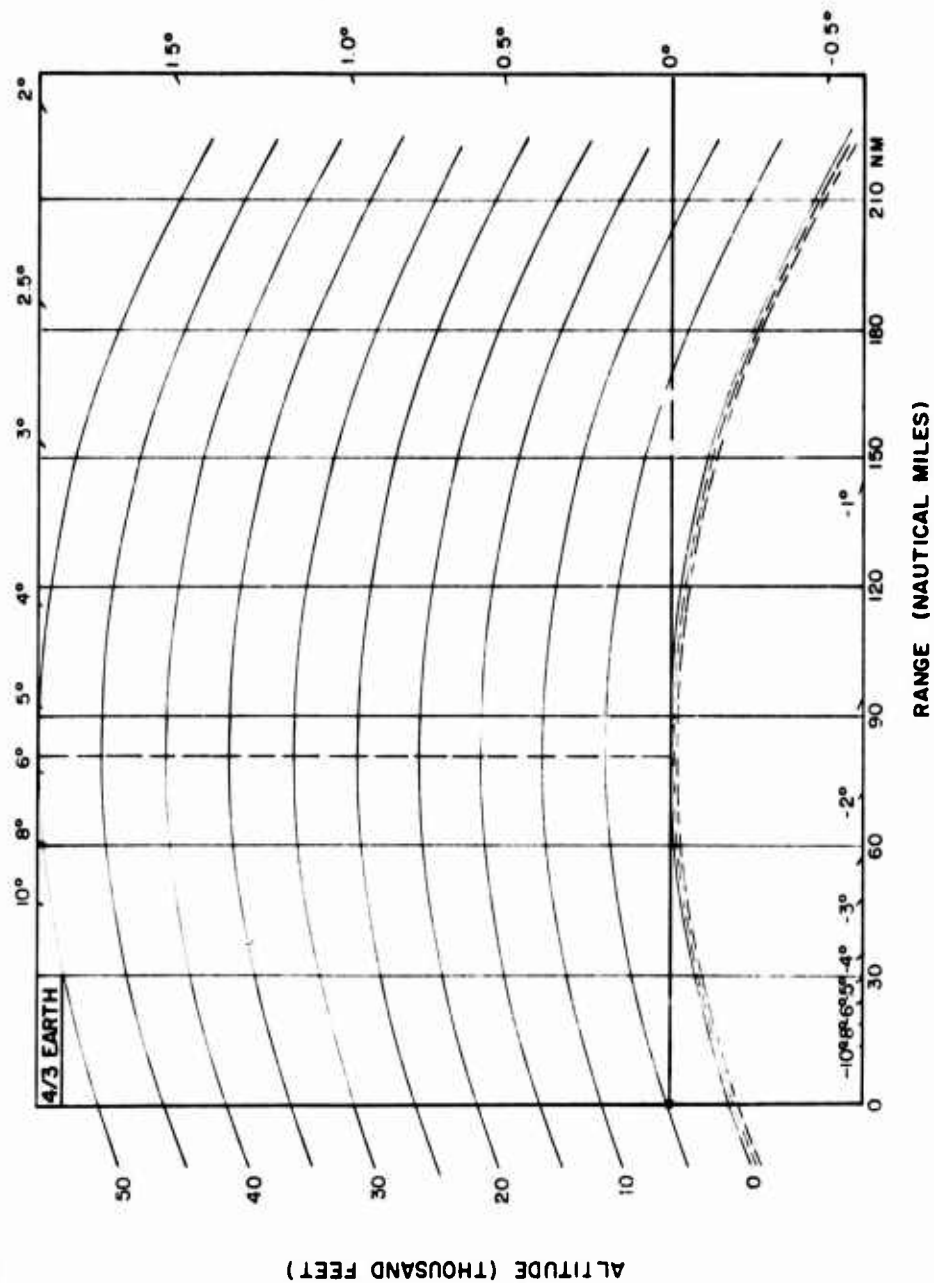


Figure 12.0 EARTH GEOMETRY (AIRCRAFT AT 4.4 K FT.)

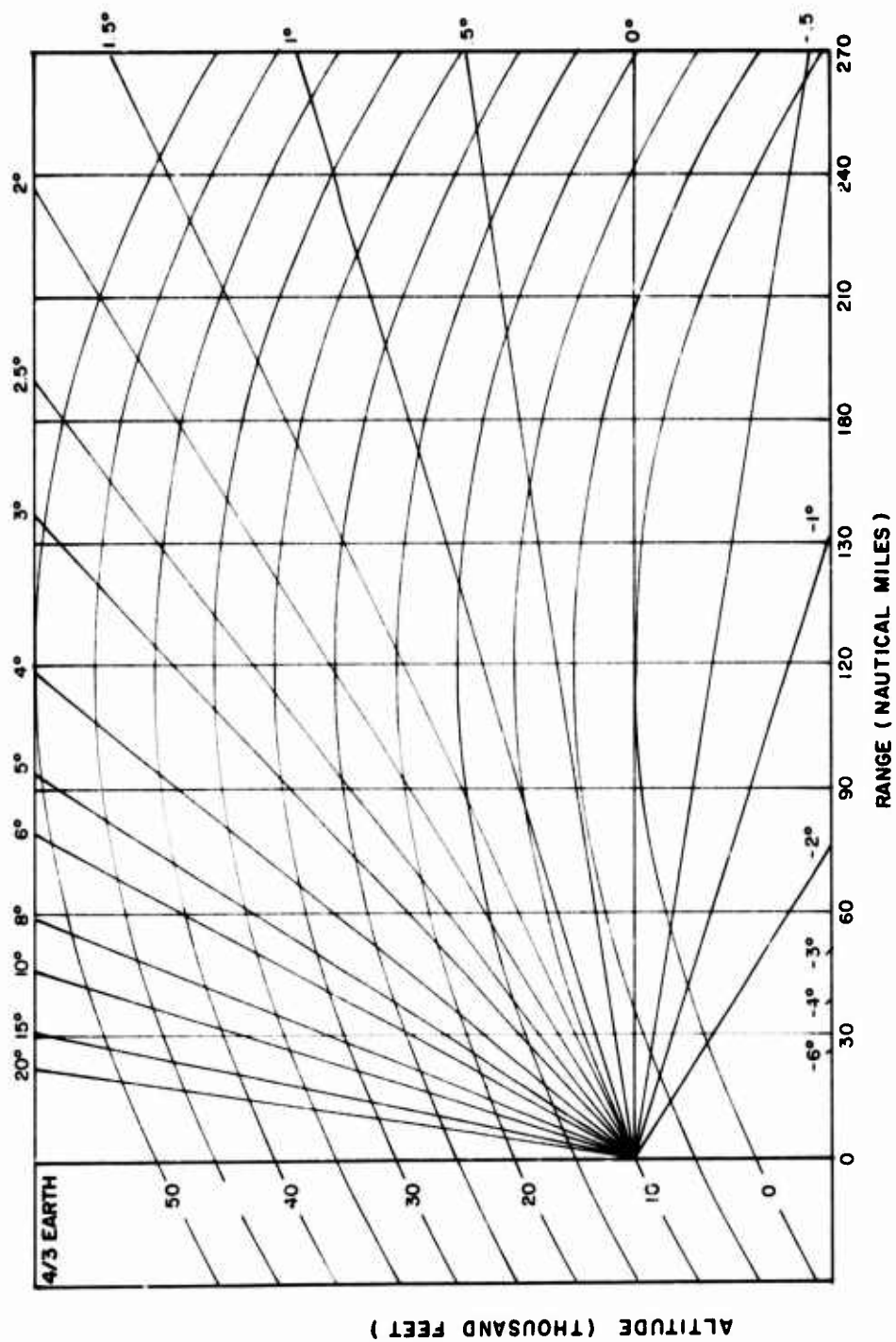


Figure 13.0 ELEVATION LOOK ANGLE AND ALTITUDE VERSUS RANGE (A/C AT 10K FT)



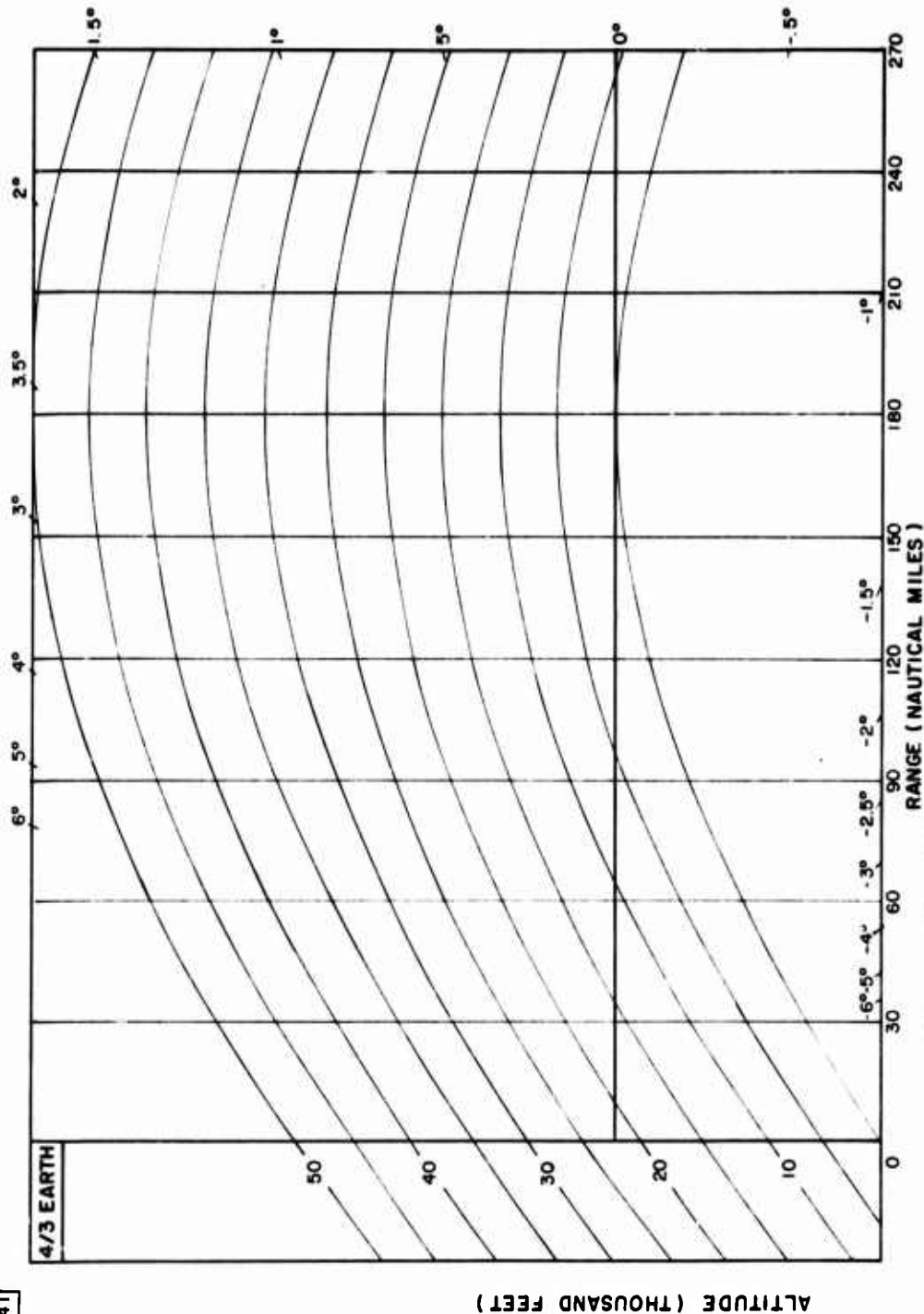


Figure 14.0 EARTH GEOMETRY-AIRCRAFT AT 22K FT

To determine effects on beam fill factor with changes in the vertical antenna beamwidth, assume the aircraft is at 10,000 feet altitude (Figure 15 illustrates this geometry). The antenna boresight look angle is one degree above the radar horizon and a storm height of 30,000 feet is assumed at a range of 120 nautical miles. We will allow the vertical beamwidth  $\theta_3$  to increase from  $2^\circ$  to  $6^\circ$  in two degree steps. Figure 15 shows the top of the storm  $1.35$  degrees ( $\phi^+ = +1.35^\circ$ ) above the boresight and the ground shades the bottom part of the beam one degree ( $\phi^- = -1.0^\circ$ ) below the boresight axis. With these angles the percentage of power intercepted by the cloud can be determined from Figure 10. We are assuming the storm is much wider than the antenna azimuth beamwidth. Table I below shows the results of these calculations.

$\theta_3$	$\phi^+$	$\phi^+ / \theta_3$	Cloud Height		$\phi^-$	$\phi^- / \theta_3$	Earth Shading BFF %	Total BFF	
			%	dB				%	dB
$2^\circ$	1.35	.675	96	- .2	$1.0^\circ$	.5	7.5	88.5	- .56
$4^\circ$	1.35	.338	82	- .9	$1.0^\circ$	.25	24.0	58	-2.36
$6^\circ$	1.35	.225	73	-1.4	$1.0^\circ$	.167	32.0	41	-3.86

TABLE I

#### EXAMPLE OF BEAM FILLING FACTORS

The  $\phi^+$  and  $\phi^-$  are used to designate portions of the beam subtended by storm height and earth shaded area.  $BFF^+$  and  $BFF^-$  are the corresponding beam fill factors. Total BFF is determined by subtracting  $BFF^-$  from  $BFF^+$ . It must be pointed out that the portion of BFF which is due to shading by the earth can be determined from aircraft position and beam geometry and, therefore, signal returns can be compensated for this portion of the BFF. However, since the height

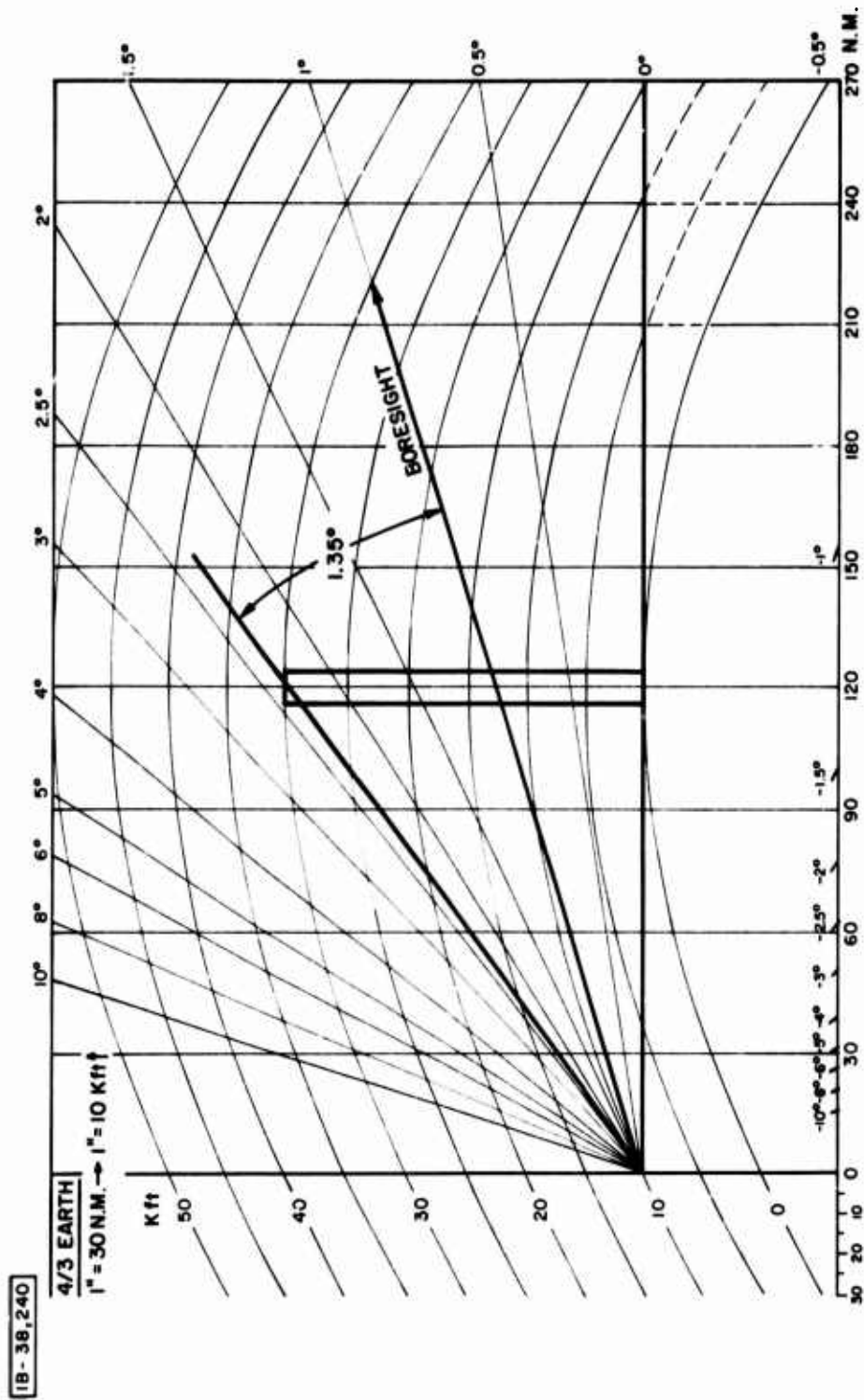


Figure 15.0 STORM HEIGHT GEOMETRY

of the storm is not known, that portion of the BFF caused by cloud height cannot be compensated for in the signal return. Note that as the vertical beamwidth increases from  $2^\circ$  to  $6^\circ$  the BFF due to cloud height varies from -0.2 dB to -1.4 dB. If the cloud height should be only 20,000 feet, the corresponding BFF values would vary from -1.2 to -2.3 dB. Evidently, all other things being equal, greater cloud heights tend to increase the BFF.

The cloud height BFF is an indirect measure of error in measuring rainfall rate. At non-attenuating wavelengths (below 3000 MHz) for every dB below zero of BFF, the error in measuring rain rate is approximately 0.7 dB. This result is derived from Equation 11 where  $Z = 289 \text{ RR}^{1.4}$ . Solving for the rain rate:

$$\text{RR} = \left( \frac{Z}{289} \right)^{\frac{1}{1.4}} = \frac{Z}{160}^{0.715}$$

Taking logs of both sides,  $\log \text{RR} = (0.715 \log Z) - \log 160$   
and differentiating  $d(\log \text{RR}) = 0.715 d(\log Z)$

$$\frac{d(\log \text{RR})}{d(\log Z)} = 0.715$$

Log RR and log Z are proportional to RR and Z when the latter are expressed in decibels.

While Equation (11) is the expression preferred by NHC for use with hurricane rain, other radar observations of rainfall have resulted in exponents of RR varying from 1.38 to 1.6. The rate of change of RR per dB of Z can thus vary from 0.73 to 0.63 dB. A calculation of rain rate error in percent versus variation in BFF (for non-attenuating wavelengths) is shown in Figure 16. From this figure we see that a BFF of -2.3 dB will make the measured rain rate appear to

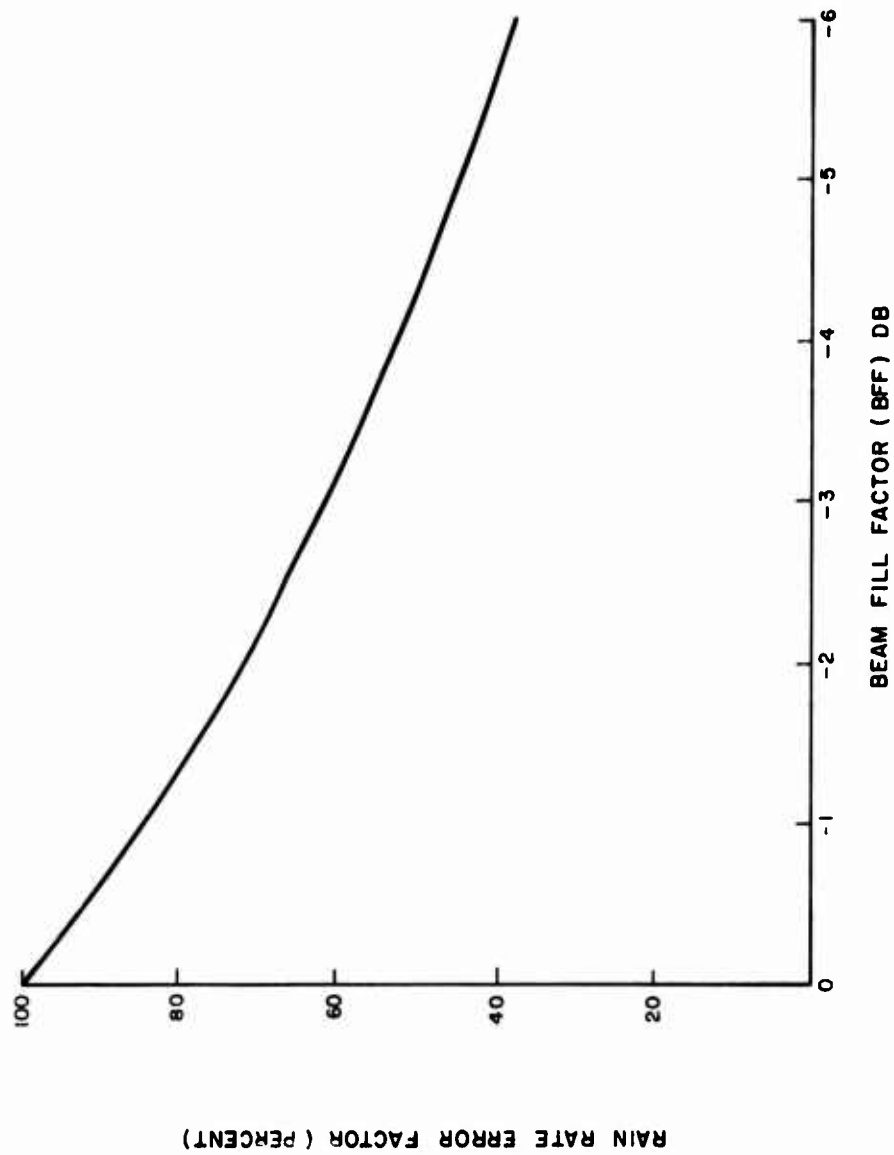


Figure 16.0 RAIN RATE ERROR FACTOR VERSUS BFF  
( FOR NON ATTENUATING WAVELENGTHS )

be 69% of the correct value. Once the allowable error in rain rate measurements is established taking all factors (including attenuation) into consideration, Figure 16 can be used to establish a minimum tolerable BFF. Later in this report we will show the effect of BFF on the estimation of rain rate when an attenuating wavelength is utilized.

It must be remembered that the above derivation pertains to non-attenuating wavelengths. If the SEEK STORM radar is to utilize a wavelength which is attenuated by rain then the main error contribution due to BFF will be in the estimation of attenuation which will severely affect estimates of rain intensity. The reason for this is that any technique which attempts to correct for attenuation and thus obtain a better estimate of reflectivity to get rain intensity must determine how much attenuation is encountered as the beam propagates in and out of the storm cells. If the total beam is not filled the estimate of attenuation will be in error which will create larger errors in attenuation correction with attendant large error in reflectivity estimates and rain intensity.

### 3.1.2.2 Beam Integration Factors and Beam Depression Factor

To express the signal-to-clutter ratio under more realistic conditions than used to write Equation 14 we must use more rigorous mathematics. Figure 17 illustrates the geometry. This is a cross section view of the beam pattern which is assumed to be circular. The angles  $\theta^+$  and  $\theta^-$  are the angles from boresight to the top of the storm and the sea surface. The angle  $\theta_c$  is that azimuth portion of the beam which is subtended by the sea surface. Equation 14 must now be written as:

$$\frac{S}{C} = \frac{\eta R \int_{\theta^-}^{\theta^+} \int_{-\theta(\varphi)}^{\theta(\varphi)} G^2(\theta, \varphi) d\theta d\varphi}{\sigma^0 \int_{-\frac{\theta_c}{2}}^{+\frac{\theta_c}{2}} G^2(\theta; \varphi^-) d\theta} \quad (15)$$

The double integration in the numerator represents the summation of all two-way beam power subtended by the rain clouds. The denominator represents the integration of that part of the beam power intercepted by the sea surface at  $\varphi^-$ . In order to obtain normalization of this equation which will facilitate numerical integration and eliminate the necessity for including absolute power, this equation can be written as:

$$\frac{S}{C} = \frac{\eta R \left[ G^2(0, 0) \right] \left[ \frac{\iint G^2(\theta, \varphi) d\theta d\varphi}{G^2(0, 0)} \right]}{\sigma^0 \left[ G^2(0, 0) \right] \left[ \frac{G^2(0; \varphi^-)}{G^2(0, 0)} \right] \left[ \frac{\int G^2(\theta; \varphi^-) d\theta}{G^2(0; \varphi^-)} \right]} \quad (16)$$

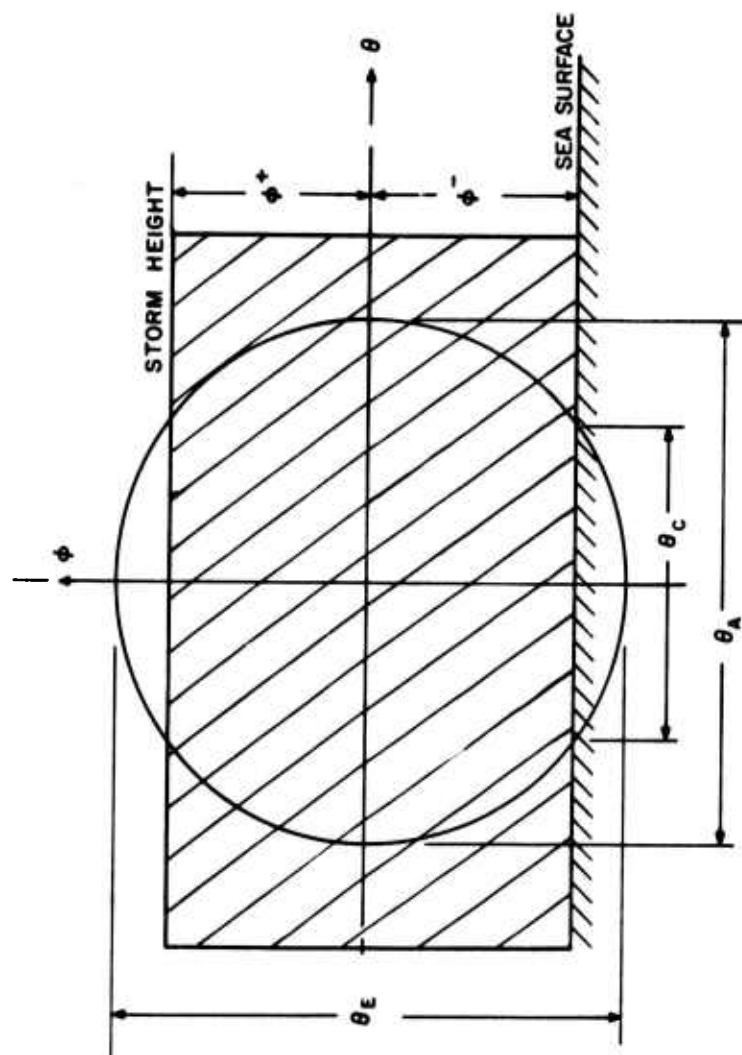


Figure 17.0 SIGNAL TO CLUTTER GEOMETRY



which can be reduced by notation to:

$$\frac{S}{C} = \frac{\eta R (BIF_1) (\theta_3)^6}{\sigma^0 (BDF) (BIF_2)} \quad (17)$$

$BIF_1$  and  $BIF_2$  can be called beam integration factors and BDF is called the beam depression factor.  $BIF_1$  is a factor which represents that part of the total beam power which is subtended by the rain cloud normalized to the antenna gain at boresight all on a two-way basis.  $BIF_2$  is a factor which represents that part of the beam power which is intercepted by the sea surface at  $\theta^-$ , normalized to the antenna beam power at zero degrees azimuth and  $\theta^-$  elevation. The BDF is a factor which normalizes the beam power at zero degrees azimuth and  $\theta^-$  to the beam power at boresight. Calculations of the factors  $BIF_1$ ,  $BIF_2$ , and BDF have been performed and the results are shown in Figures 18, 19, and 20. For each of these curves the angle  $\theta$  has been normalized to the -3dB one-way antenna beamwidth. For this reason the angle  $\theta_3$  has been added to Equation 17 to denormalize the factors. This allows the curves to be utilized for any beamwidth of interest. The integration was performed on the beam pattern shown in Figure 2.

These results will allow calculations of signal-to-clutter ratios. We will assume the same conditions as previously. Namely, range is 120 nautical miles, aircraft altitude is 10,000 feet, cloud height of 30,000 feet, a boresight look angle of  $+1^\circ$  and a vertical beamwidth varying from  $2^\circ$  to  $6^\circ$  in  $2^\circ$  increments. Figure 15 illustrates the geometry. A rain rate of 10 millimeters per hour will also be assumed and the S/C calculation will be performed for frequencies of 3000 megahertz ( $\lambda = 10$  cm) and 5000 megahertz ( $\lambda = 6$  cm).

---

<sup>6</sup>  $\theta_3$  in this equation is the elevation 3 dB beamwidth.

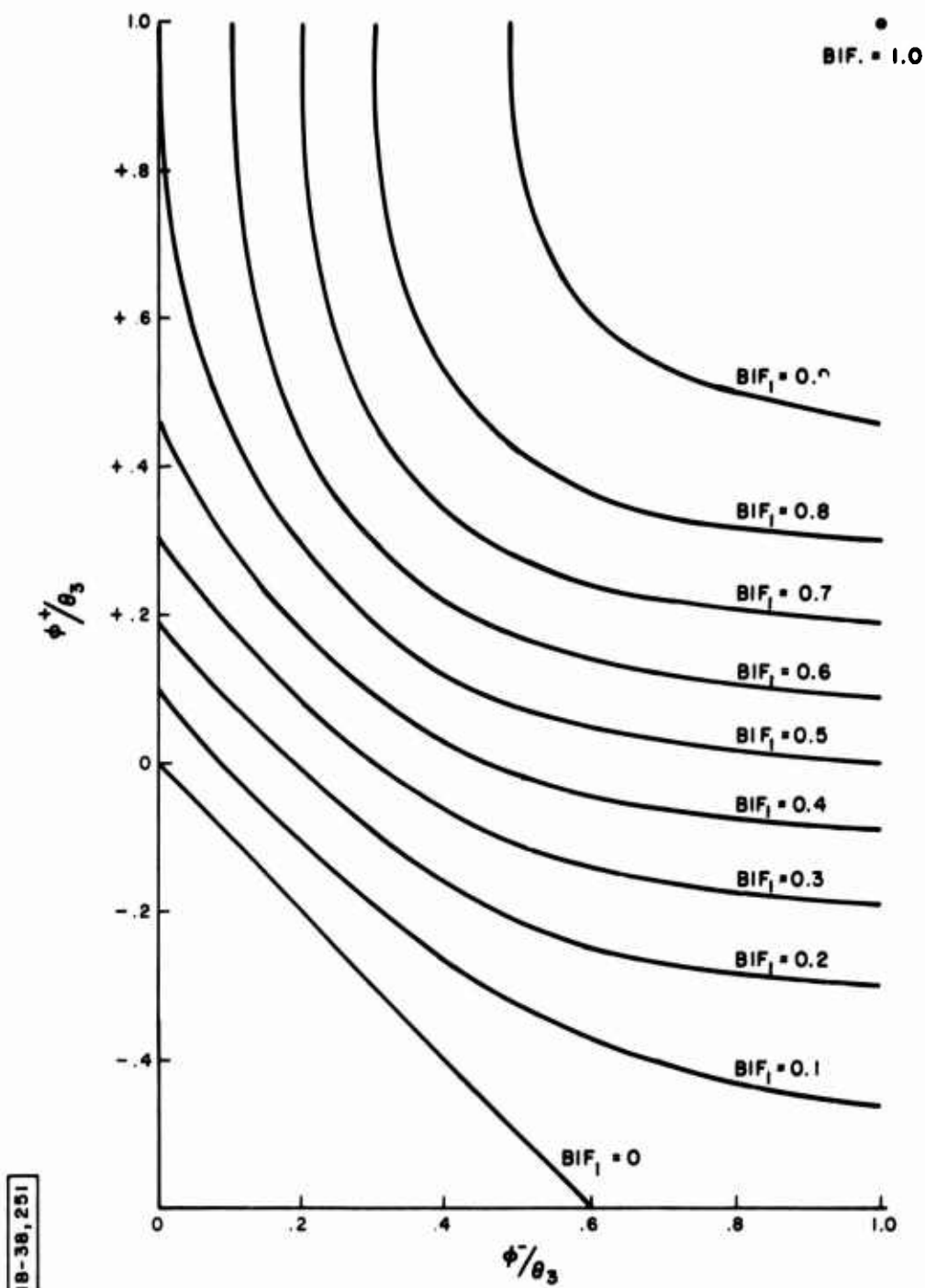


Figure 18.0  $BIF_1$  VERSUS NORMALIZED BEAM ANGLES

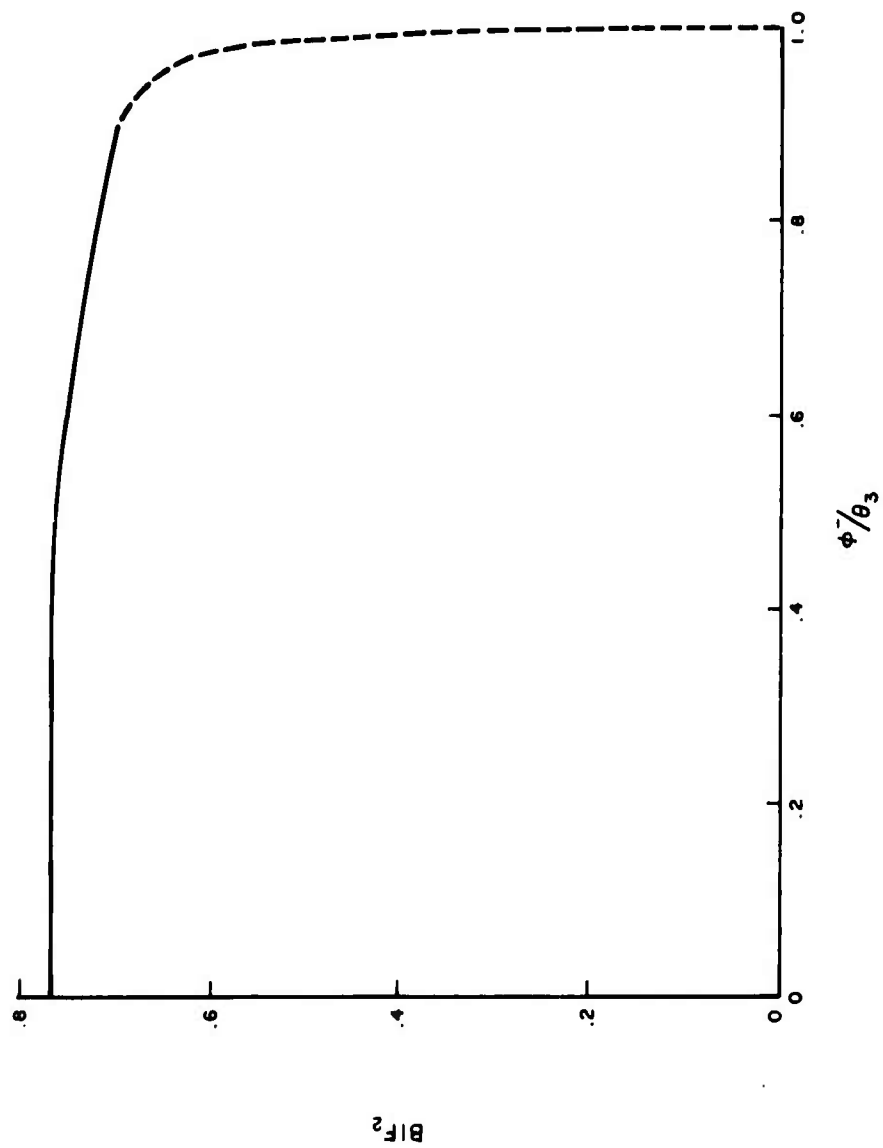


Figure 19.0  $BIF_2$  VERSUS NORMALIZED  $\phi^-$

1A-38,237

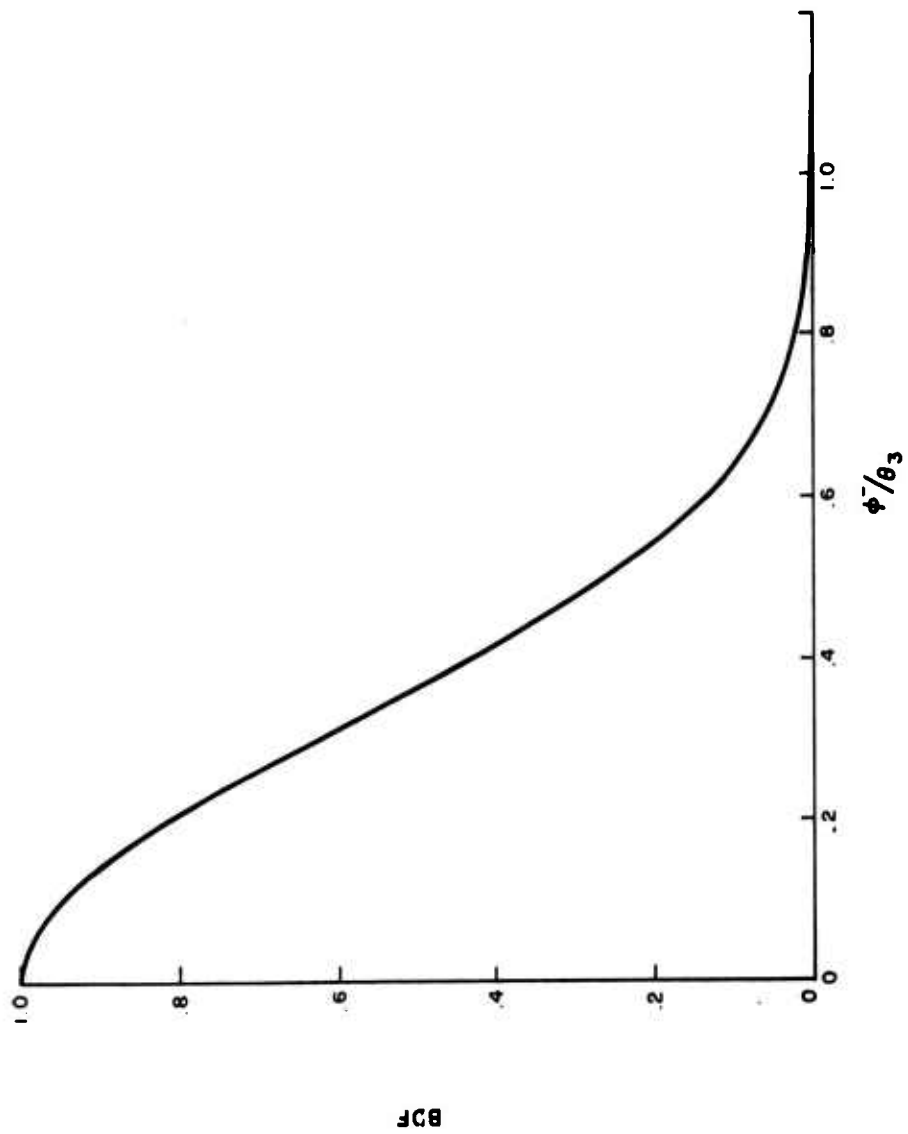


Figure 20.0 BEAM DEPRESSION FACTOR VERSUS NORMALIZED DEPRESSION ANGLE

Figure 8 indicates a radar reflectivity ( $\eta$ ) of  $-77 \text{ dB/m}^{-1}$  for 10 centimeters wavelength and  $-68 \text{ dB/m}^{-1}$  for 6 centimeter wavelength at a rain rate of 10 mm/hr. Equation 17 can now be used with the aid of Figures 18, 19, and 20 to determine the S/C ratios. As previously mentioned a value of  $-40 \text{ dB}$  will be used for  $\sigma^0$ . Table II shows the results of these calculations.

$\theta_3$	$\text{BIF}_1$	$\text{BIF}_2$	BDF	5000 MHz S/C (DB)	3000 MHz S/C (DB)
$2^\circ$	.83	.76	.26	18.35	9.35
$4^\circ$	.50	.76	.73	13.65	4.65
$6^\circ$	.37	.76	.86	13.42	4.42

TABLE II  
SIGNAL TO CLUTTER VERSUS BEAMWIDTH AND FREQUENCY

These results indicate fairly acceptable values of S/C at C-Band but not acceptable at S-Band which indicates that clutter can be a serious problem for the SEEK STORM radar. For the example shown the storm is assumed to be infinite in azimuth. Therefore, the variation in S/C ratio as the beamwidth increases does not depend only upon non-beam filling in elevation but also on the increasing azimuth extent of the storm. To appreciate the effect ground clutter has upon rain rate estimates let us calculate an equivalent reflectivity for the sea clutter and equate this to rain reflectivity. Equation 17 can be written as:

$$\frac{S}{C} = \frac{Z_R (BIF_1)}{Z_C} \quad (18)$$

where  $Z_R$  is the actual rain reflectivity and the product  $Z_R (BIF_1)$  represents the radar measured rain reflectivity.  $Z_C$  is the equivalent rain reflectivity of the clutter assuming a full beam filling situation.

For a rain rate of 10 mm/hr the reflectivity of rain from Figure 9.0 is  $Z_R = 7000$ . If we take the S/C values for the  $6^\circ$  beamwidth case shown in Table II which have a  $BIF_1$  of .37, calculations of equivalent reflectivities ( $Z_C$ ) at 5000 and 3000 MHz can be performed using Equation 18. At 5000 MHz the equivalent  $Z_C$  is 118 and at 3300 MHz the  $Z_C$  is 940. From Figure 9.0 these are equivalent to rain rates of 0.3 and 2.4 mm/hr.

From the conditions calculated the results appear to indicate that signal-to-clutter could be expected to present some problems in rain rate estimation particularly at S-Band. As previously stated attenuation effects could also cause large errors in rain rate estimation because clutter returns will be interpreted as rain and therefore be used to estimate erroneously total path attenuation. This does not appear to be a problem, however, since attenuation at 5000 MHz for rain rates in the order of 0.3 mm/hr is only .001 dB/NM. If there were 100 nautical miles of sea clutter this would cause an error in attenuation estimation of only 0.1 dB. Attenuation of 2.4 mm/hr at 3000 MHz over a path length of 100 nautical miles is also about .1 dB.

To see how signal to clutter varies as the boresight angle is depressed from a relatively high elevation angle toward the earth tangent refer to Figure 21.0. This set of curves was calculated using Equation 17 and Figures 18, 19, and 20. The calculations assumed similar conditions as previously. ( $\theta_3 = 2^\circ$ ,  $R = 120 \text{ NM}$ ,  $\sigma^0 = -40 \text{ dB}$ ,  $\eta = -68 \text{ dB}$  at 5000 MHz and  $\eta = -77 \text{ dB}$  at 3000 MHz.) Note that in both cases as the elevation angle is increased the S/C also increases. The curves become asymptotic at a point where the effective beam power is no longer illuminating the sea surface. At low elevation look angles the S/C ratio is the lowest value. It is apparent that a minimum elevation beamwidth is only necessary to insure that the beam is filled with rain clouds and that ground clutter should not be considered an influencing factor for selection of elevation beamwidth.

### 3.2 Horizontal Antenna Beamwidth

Beamwidth of the antenna pattern in the horizontal plane is determined from azimuth resolution requirements and the target rain cloud characteristics. In the SEEK STORM radar a hurricane eye must be detected and resolved at relatively long distances. In order to arrive at a basic quantitative understanding of the antenna azimuth beamwidth requirements, a hurricane model similar to that shown in Figure 5.0 is postulated and this is used to investigate azimuth beamwidth.

#### 3.2.1 Beamwidth versus Angular Resolution

The storm eye is assumed to have a radar reflectivity of zero. The surrounding eye wall is wider in azimuth than the entire radar beam. The eye wall reflectivity is constant and sufficiently large

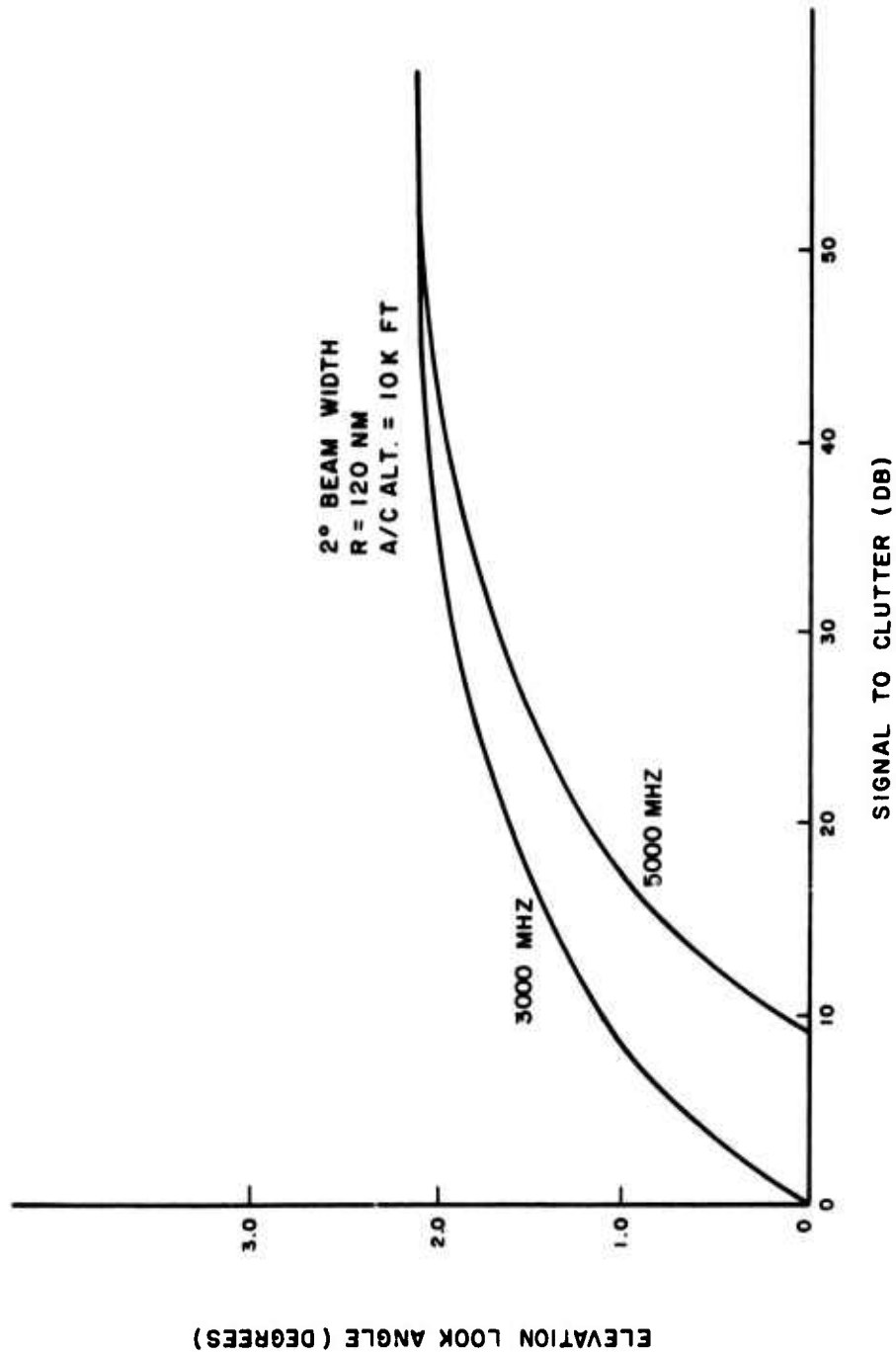


Figure 21.0 SIGNAL TO CLUTTER VERSUS ELEVATION LOOK ANGLE



so that some maximum signal level will be assumed when the entire radar beam is intercepted by the eye wall. The radar pulse length is very much smaller than the diameter of the eye.

The signal received at the radar when the antenna beam is entirely filled by rain in the eye wall, will be taken as the return signal reference (zero decibels). As the beam scans in azimuth toward the center of the eye, larger and larger parts of the beam will be intercepted by the eye. Since the eye returns no power (by definition: zero reflection coefficient) the total received power will tend to decrease until the antenna boresight axis points at the center of the eye. At this point in the scan, minimum energy is received. If the scan is continued in the same direction, the received power will increase until it again reaches zero decibels.

The antenna beam energy pattern shown in Figure 10 will also be used in this portion of the study. As a reference the "effective azimuth beamwidth" ( $\theta_{\text{eff}}$ ) will be defined as that beamwidth in which 99 percent of the total two-way power resides within the beam pattern. For the antenna pattern chosen in this study,  $\theta_{\text{eff}} = 2.24 \theta_3$ , where  $\theta_3$  is the 3 dB beamwidth.

As a starting point, the diameter of a hurricane eye will be assumed to subtend an angle ( $\epsilon$ ) which is smaller than the 3 dB azimuth beamwidth. Let  $\epsilon = .36\theta_{\text{eff}}$ , i.e., ( $\epsilon = 0.8\theta_3$ ), Figure 22 (a) through 22 (f) illustrate this beam position relative to a hurricane eye wall as the beam is moved from the center of the eye toward the left. This angle has been normalized with respect to  $\theta_3$  so that results can be applied to any 3 dB beamwidth.

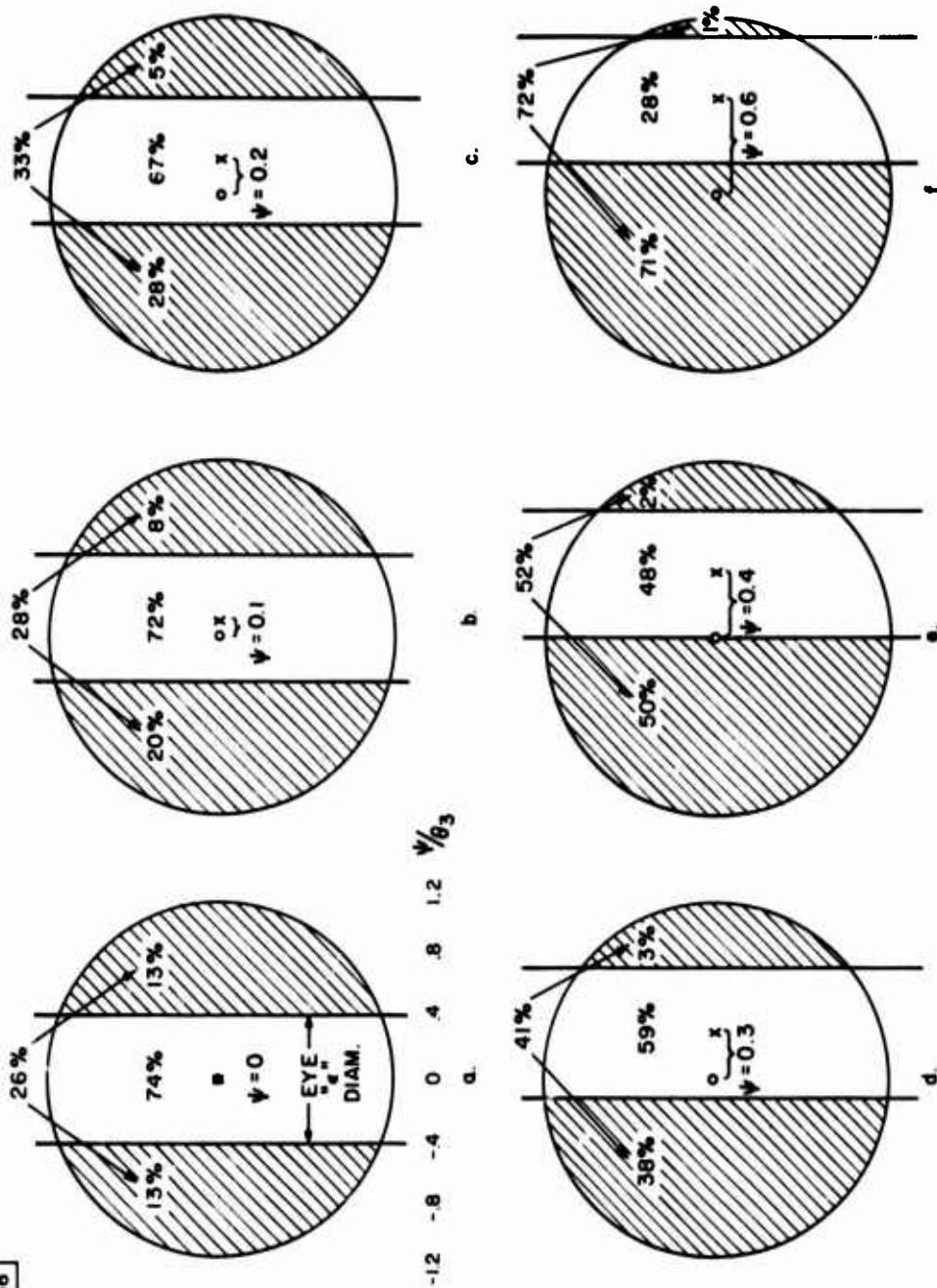
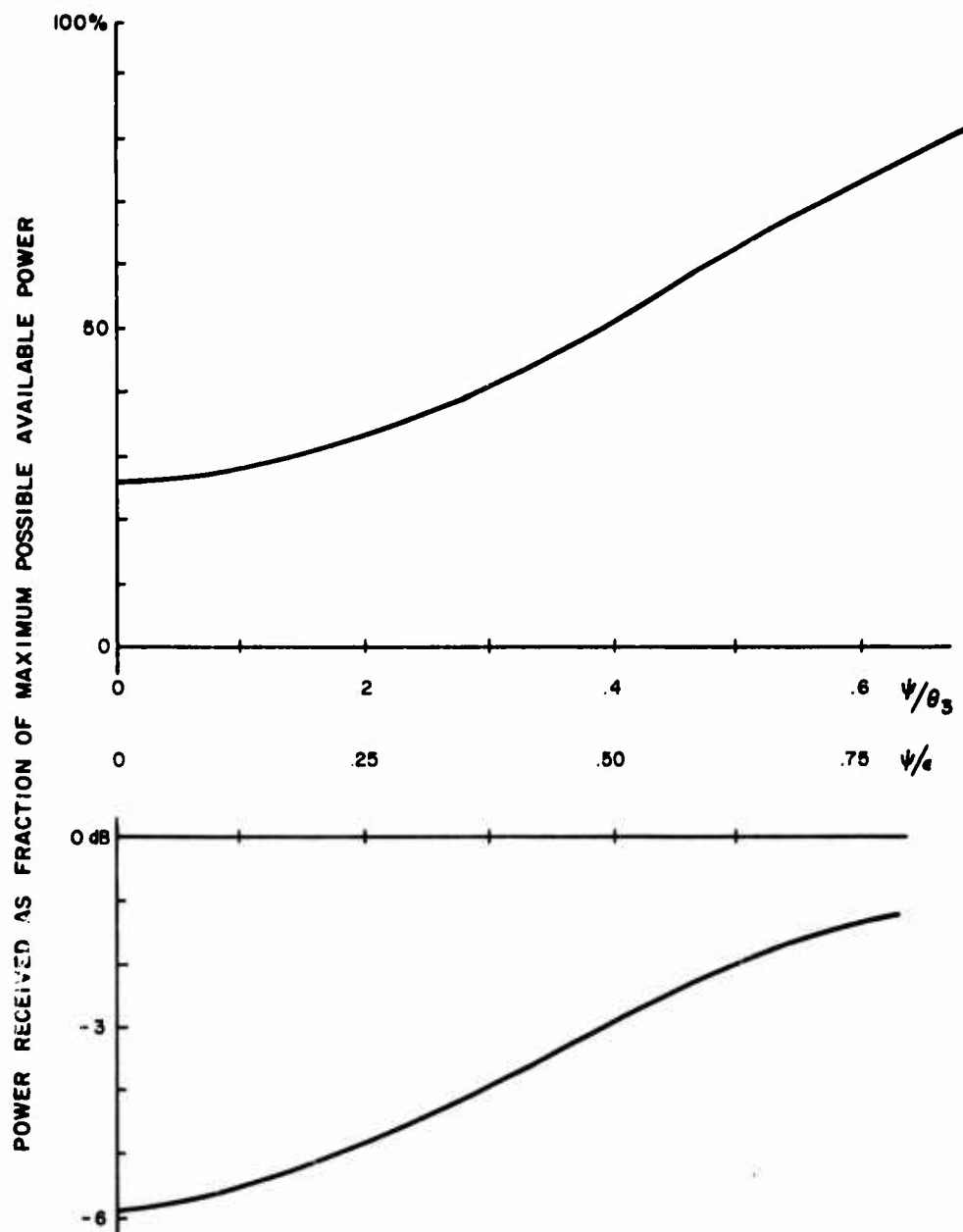


Figure 22.0 BEAM POSITION RELATIVE TO HURRICANE EYE

Percentage of two-way power for the various portions of the beam pattern have been determined from Figure 10 and are also shown for each beam position. The amount of power received from the eye walls as a percent of the total power available has been plotted in Figure 23 as a function of beam position. Beam position ( $\psi$ ) has been expressed in terms of the 3 dB beamwidth  $\theta_3$  and the angular extent of the eye diameter ( $\epsilon$ ). In the lower part of Figure 23 the same curve is plotted in decibels. Note that for this example (i.e., when the storm eye is smaller than the effective beamwidth  $\theta_{\text{eff}}$ ) a null at the center of the eye would only be about 6 dB down from a signal which would be received if the entire beam were subtended by rain in the eye wall. A 6 dB null is not considered very acceptable for detection of hurricane centers. A 10 to 20 dB null will more likely be required.

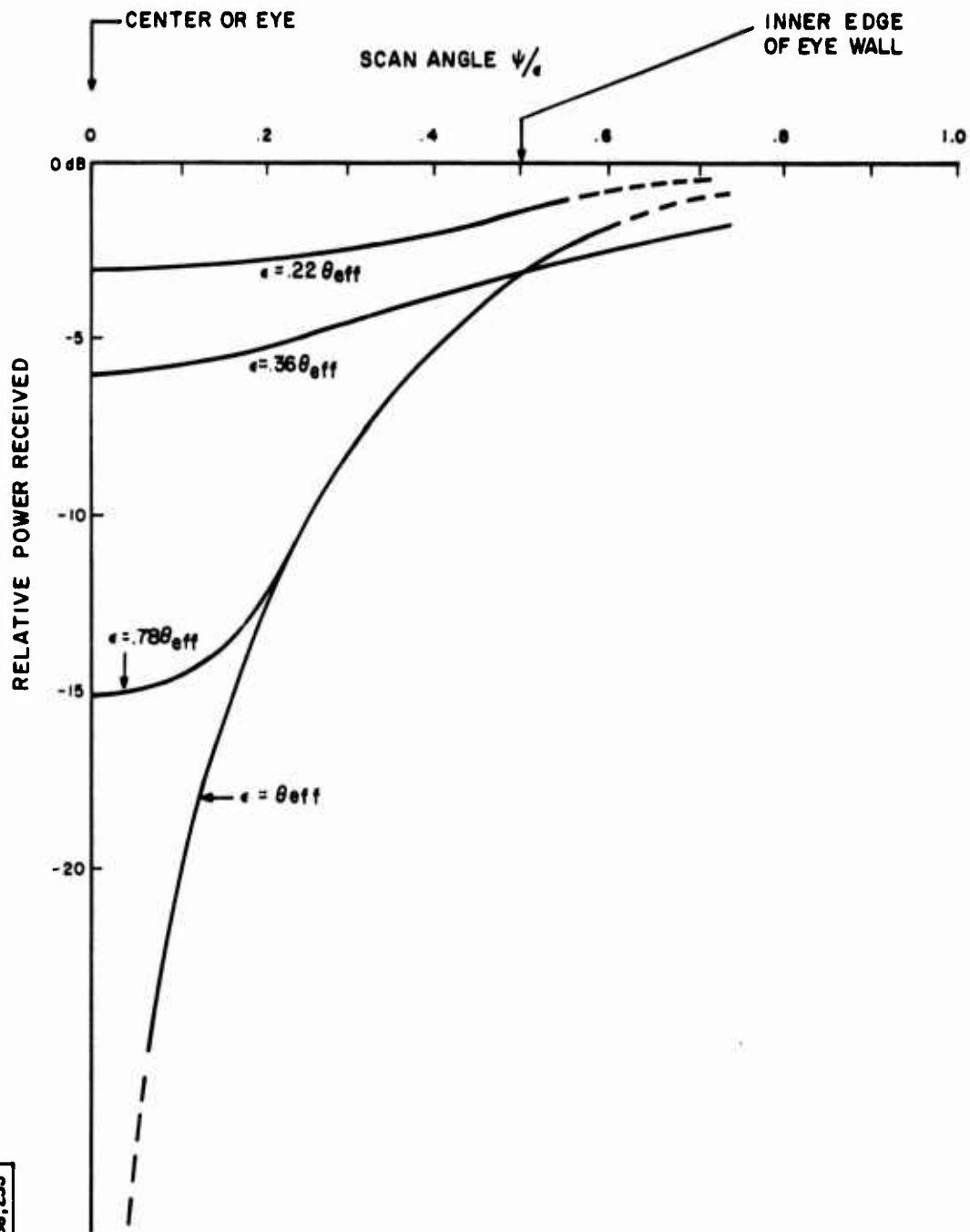
Similar calculations have been performed for cases where  $\epsilon = \theta_{\text{eff}}$  and  $\epsilon \gg \theta_{\text{eff}}$ . Results of all these calculations are shown in Figure 24. Note that as we scan through the hurricane eye a very deep null will be obtained if the angle subtended by the eye diameter  $\epsilon$  is greater than or equal to the effective beamwidth. If the effective beamwidth overlaps the eye diameter by only 25% the null is about 15 dB.

To show how this null varies with the 3 dB antenna beamwidth refer to Figure 25. A -15 to -20 dB null would require the normalized 3 dB beamwidth to be about 0.5, ( $\frac{\theta_3}{\epsilon} = 0.5$ ). Figure 26 is a curve of range versus  $\epsilon$  for a 10 nautical mile hurricane eye diameter. This curve shows that  $\epsilon$  at 150 nautical miles would be 3.8 degrees. If this angle is used in the above relation, ( $\frac{\theta_3}{\epsilon} = 0.5$ ). A 3 dB beamwidth ( $\theta_3$ ) of 1.9 degrees would be required to obtain a -15 to -20 dB null from a 10 nautical mile diameter eye at a 150 nautical mile range. This means that the SEEK STORM radar azimuth angular beamwidth should be designed to be less than 2 degrees and smaller if possible because



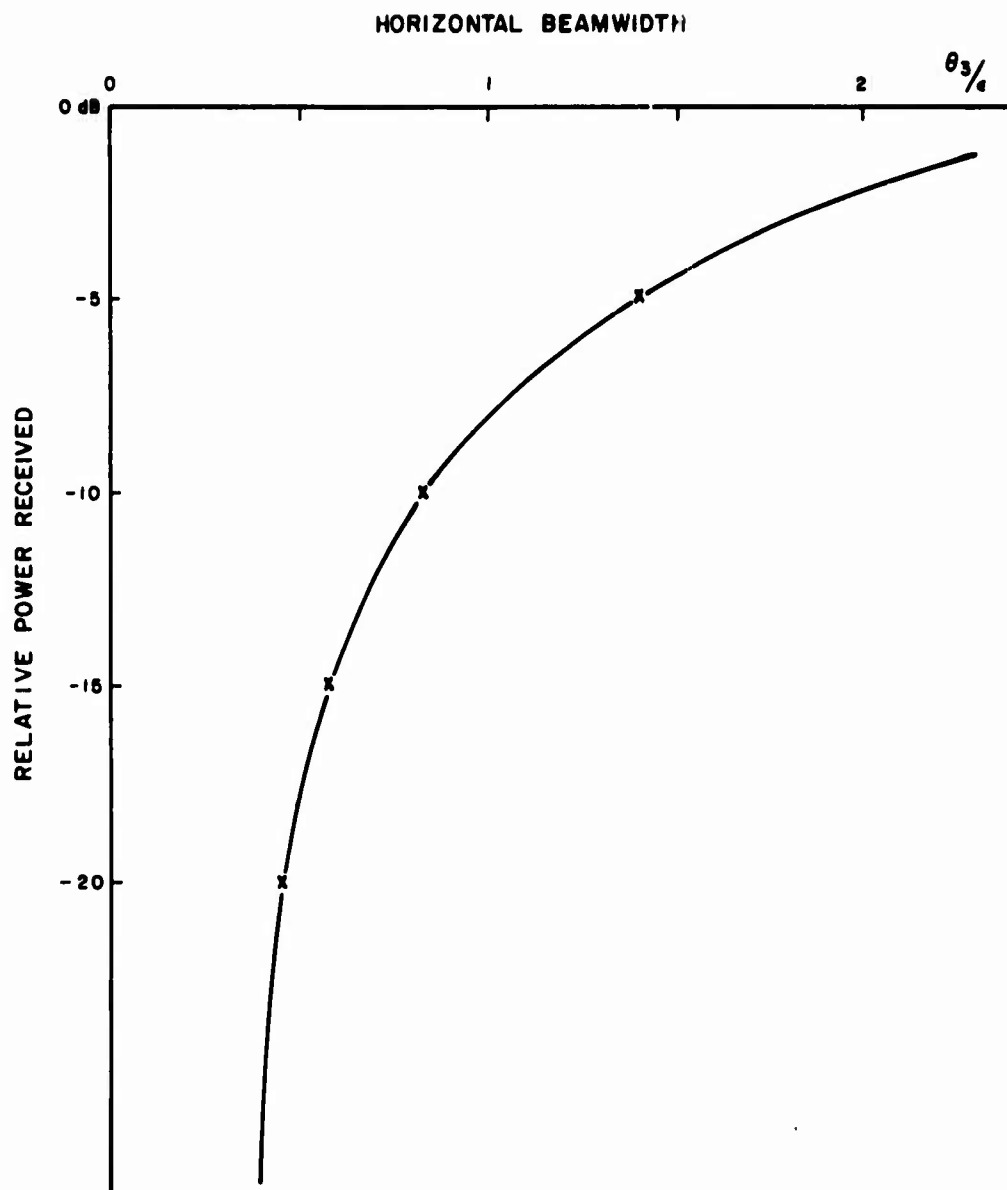
1B-38,234

Figure 23.0 RELATIVE POWER VERSUS BEAM POSITION



1A-38,255

Figure 24.0 RELATIVE POWER VERSUS SCAN ANGLE



IA-38,256

Figure 25.0 RELATIVE POWER VERSUS NORMALIZED HORIZONTAL BEAMWIDTH

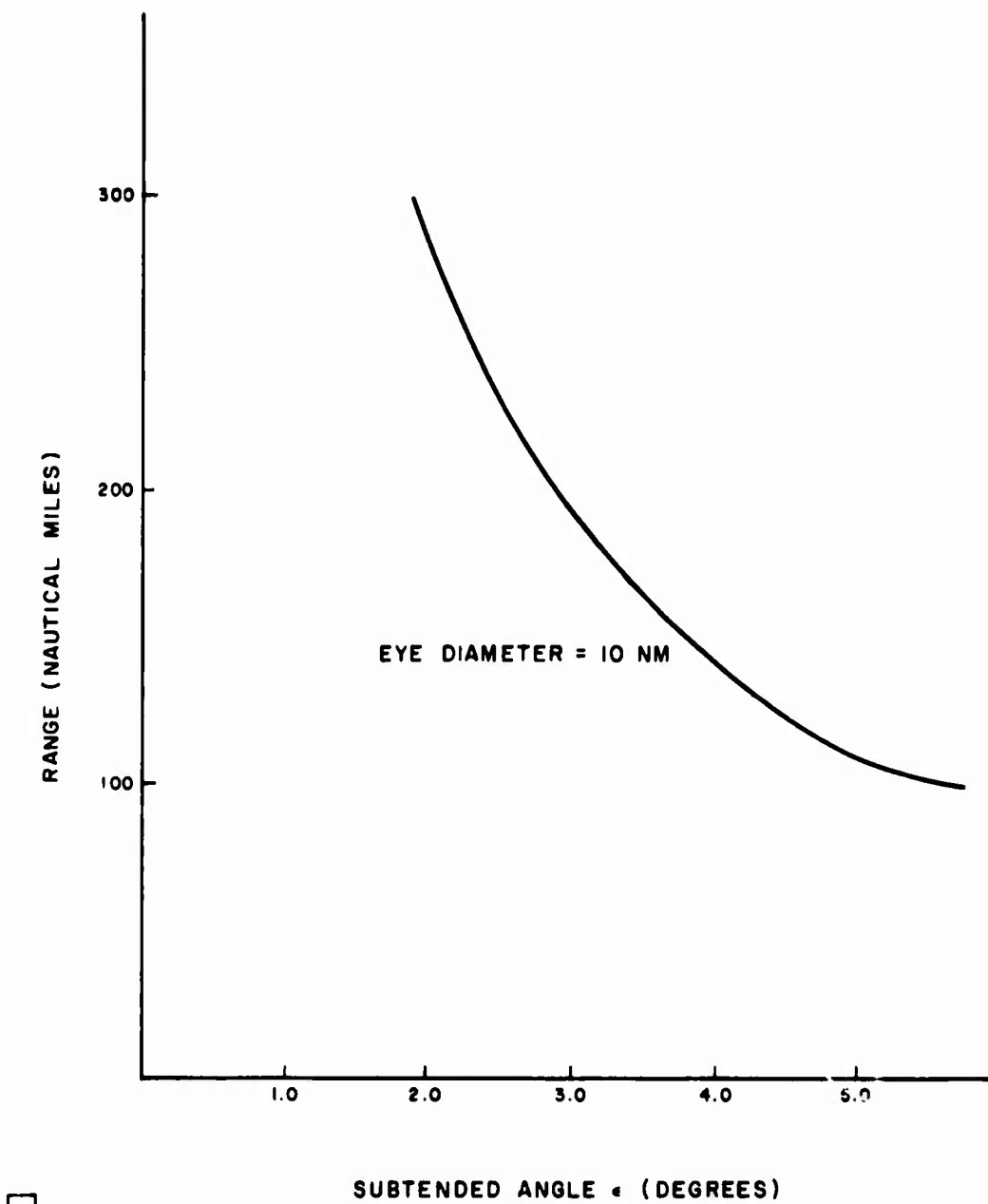


Figure 26.0 RANGE VERSUS  $\alpha$

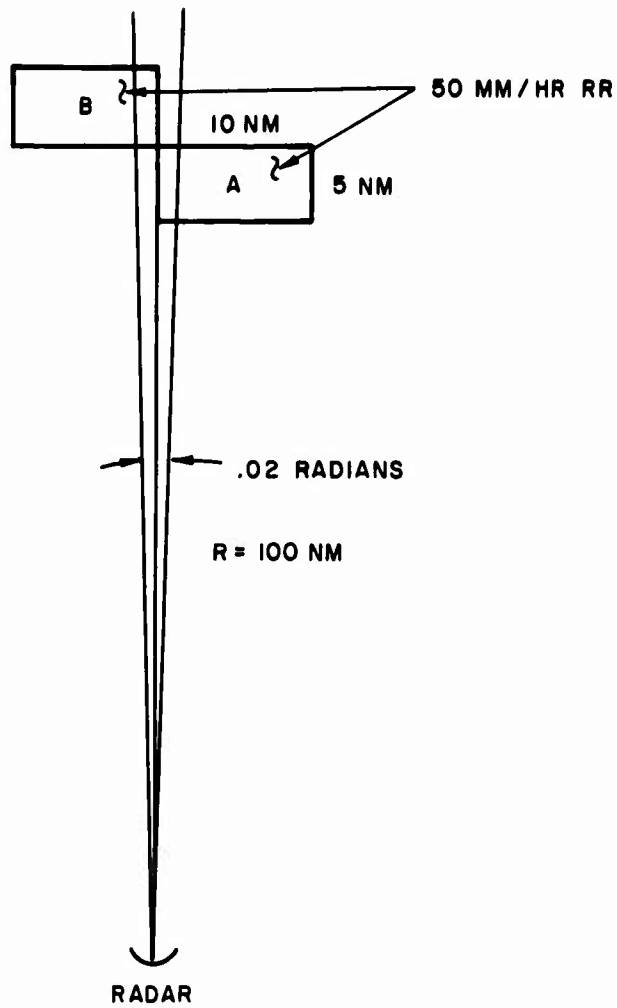
this analysis is a relatively simplified model of a true hurricane storm where side lobe levels and ground clutter are major influencing factors which have not been considered. This single model may not therefore mirror the true radar meteorological situation with sufficient realism to permit any final conclusions as to ultimate resolution capability.

Also not taken into consideration in this discussion of azimuth beamwidth is the effect of vertical BFF. Since the hurricane type storm does have a finite height to the rain walls it is obvious that at times some portions of the vertical beamwidth due to vertical beam filling will be contributing to backscatter while other portions are not. It has been shown in the discussions concerning the vertical beamwidth that errors in estimating rain rate from reflectivity factor are apparent when the beam is not uniformly filled with rain clouds. It has also been shown that as the beamwidth becomes narrower effects of BFF tend to decrease.

The effect of azimuth beamwidth on preserving the shape of a rain cell and accurately predicting rain intensity in the cell is perhaps an even greater constraint on azimuth beamwidth than the eye location requirements discussed above.

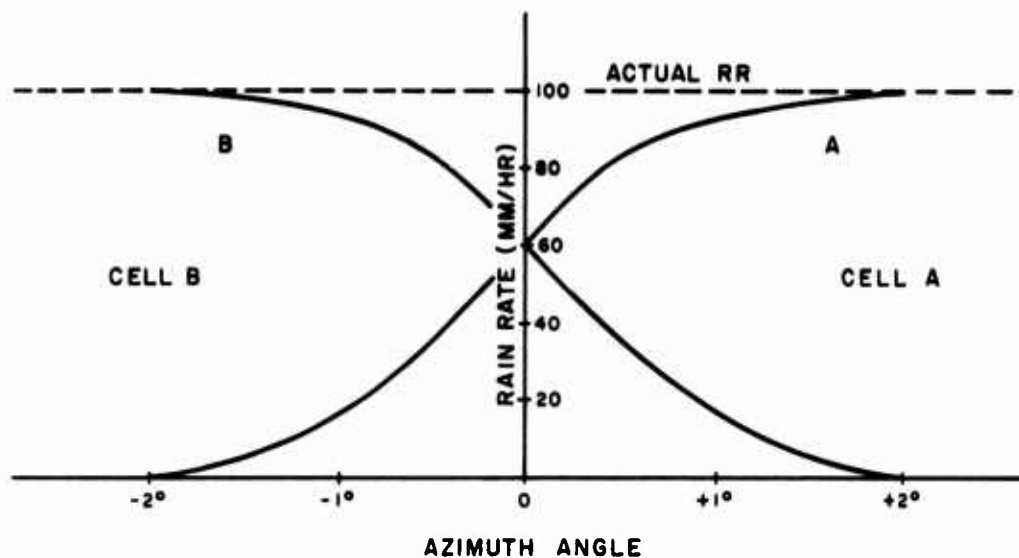
A simplified example will be given to demonstrate the problem. Figure 27 shows two rain cells (A and B) with a rain rate of 100 mm/hr at an approximate range of 100 nautical miles from the radar. The radar is assumed to have a beamwidth of 0.02 radians so that the beam extent at the range of cell A is 2 nautical miles. Figure 28(a) illustrates the radar rain rate estimate as the beam scan is azimuth. This case shows effect of azimuth smearing with no attenuation. Figure 28(b) illustrates the same with attenuation. Each one degree in azimuth represents a horizontal distance of 2 nautical miles for the case considered. The



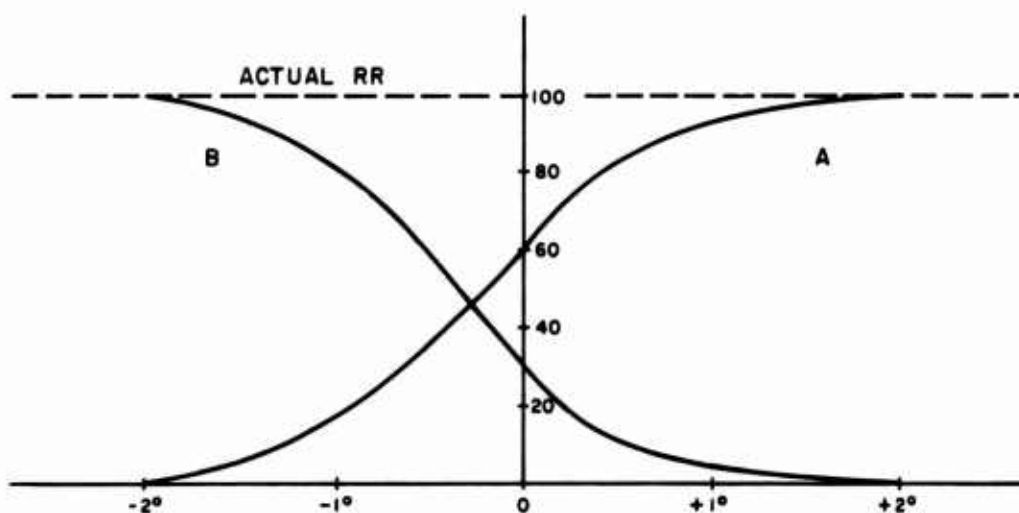


1A - 30,233

Figure 27.0 RADAR - RAIN CELL GEOMETRY



(a) RAIN RATE ESTIMATE CELL A AND B  
WITH NO ATTENUATION ( $f = 3000$  MHZ)



(b) RAIN RATE ESTIMATE CELL A AND B  
WITH ATTENUATION ( $f = 5250$  MHZ)

IA - 38, 232

Figure 28.0 AZIMUTH DISTORTION OF RAIN CELLS

steeper slope on the rain rate estimation curve for cell B in Figure 28(b) is caused by the attenuation of energy through cell A. It is obvious that the finite radar beamwidth not only distorts the external dimensions of the rain cell, but also the distribution of rain within the cell. Both of these effects tend to worsen as we estimate dimensions and rain intensities of cloud cells which are further out in range. The amount of distortion and rain rate error which result depend upon the gradient of rain rate within the cloud cells. The case considered assumes a step function of rain rate which is doubtful to exist in nature. This example however, has been presented to demonstrate another consideration which can affect resolution.

### 3.2.2 Azimuth Scan Rate versus Number of Pulses Sampled

As the antenna beam scans in azimuth pulses are being transmitted and received by the radar. The number of pulses received from the target at each instantaneous beam position and range increment can be integrated in the receiver. If enough independent samples of the rain cloud are obtained the amplitude of the integrated pulses can be related to rain intensity at the particular range increment. In the case of rain, the radar must deal with an incoherent target. This is because the configuration of the ensemble of rain drops is changing constantly as a result of the random motion of the drops with respect to each other. As a result, the backscattered power will fluctuate rapidly, in a noise-like manner.

We are, however, interested only in the average power backscattered by the rain cloud since this average power is a measure of the reflecting  $Z$  which is proportional to the rain rate  $RR$ . We cannot rely on the power average returned by one or even only a few pulses. In order to decide how many pulses and how much time are required to obtain a

meaningful average, the statistics of the echo from a large number of independent scatterers in motion must be examined.<sup>(5)</sup>

As regards the minimum time interval at which independent samples of the echo can be obtained, this is dependent upon relative motion of the rain drops and the wavelength of the radar. For C-Band, the decorrelation time is of the order of 10 milliseconds, for S-Band, about 20 milliseconds.<sup>(9)</sup> Atlas (op. cit) shows that 25 independent radar samples of a given rain volume permit calculation of the true average value of reflectivity within  $\pm 2$  dB 95% of the time. He also indicates that this is the best obtainable from a practical point of view.

Multiplying the decorrelation times cited above by 25, one arrives at sampling periods of 0.25 and 0.5 seconds for C and S-Band, respectively. From an elementary viewpoint, the beam ought to dwell on the target that long. Since a continuous scanning motion is desirable, however, let us assume the beam may move a fraction of a beamwidth (such as 1/4 beamwidth) during the time in question. If the azimuth beamwidth is 2 degrees this leads to scanning angular velocities of the order of one degree per second at S-Band or about one minute for a 60 degree scan. Should this turn out to be an undesirably long period, the sampling time can be shortened by obtaining decorrelated rain samples more quickly than by just waiting for the raindrop ensemble to "re-shuffle." Applicable methods include frequency shifting, range shifting and beam scanning.

In the frequency shift method, the transmitted wavelength is shifted between successive pulses so that the electrical length (and hence, the phase) between the individual scatterers is changed by a significant amount. It has been shown<sup>(7)</sup> that a frequency shift-pulse length product of unity is adequate. Hence, given a  $1\mu\text{s}$  pulse, a frequency shift of 1 MHz is sufficient for decorrelation.

The range shift method relies on the demonstrated fact (Atlas, op. cit) that the signals from adjacent range bins are uncorrelated. Hence, these can be used to form at least part of the required average, at the sacrifice of some range resolution. For example, if 1 nautical mile resolution is adequate, and a  $1\mu\text{s}$  pulse is used, the inherent range resolution is:  $\frac{CT}{2} = 492$  feet. Hence, a range interval of 1 nautical mile can yield  $\frac{6080}{492} \approx 12$  independent samples.

Finally, scanning the antenna beam also produces decorrelation to the extent that a part of the target scanned at one beam position vanishes from view on one side of the beam while a corresponding new part comes into view on the other side. If, for example, the beam could be moved by one whole beamwidth in one interpulse period, two successive samples, although from the same range, would be completely decorrelated.

While all three of the above techniques tend to produce independent samples, it appears that one or all methods could be utilized depending upon the particular PRF, antenna scanning velocity and azimuth map cell size which is selected. Since various investigators indicate the decorrelation time can vary from 5 to 20 milliseconds at S-Band there appears to be a considerable area for judgement in parameter selection when determining azimuth scanning rate from PRF, pulse width, the number of independent samples integrated and the number of independent samples obtained in a given time period.

A number of integrators exist or have been proposed for carrying out the required averaging process. Regardless of which combination of signal processing techniques is selected it appears that the azimuth scan rate of the SEEK STORM radar will be slow enough to require some range compensation due to relative change in aircraft position from the beginning of the scan to the end of the scan. Ultimate selection of scan rate cannot be determined until a specific signal processing approach is chosen.

### 3.3 RF Frequency

Factors affecting selection of RF frequency include attenuation (with all its resulting complications) and antenna size. Antenna size is also determined by beamwidth requirements which have been discussed. This section will discuss both attenuation and antenna size as they affect the selection of an RF frequency.

#### 3.3.1 Attenuation

A major influence on the choice of operating frequency must be the effect of attenuation due to rain clouds. Medhurst<sup>(8)</sup> has shown the attenuation per unit distance to be very strongly dependent on frequency. Figure 29 illustrates this information for various rain rates. Some of these data have been used to plot the attenuation factor ( $\alpha$ ) curve in Figure 30 from which can be read the attenuation (in decibels/kilometer) due to 50 mm/h rain in the frequency band of interest. Also shown in this figure are the variations in gain, beamwidth and wavelength assuming a 6 foot diameter antenna. Note that

18-38,250

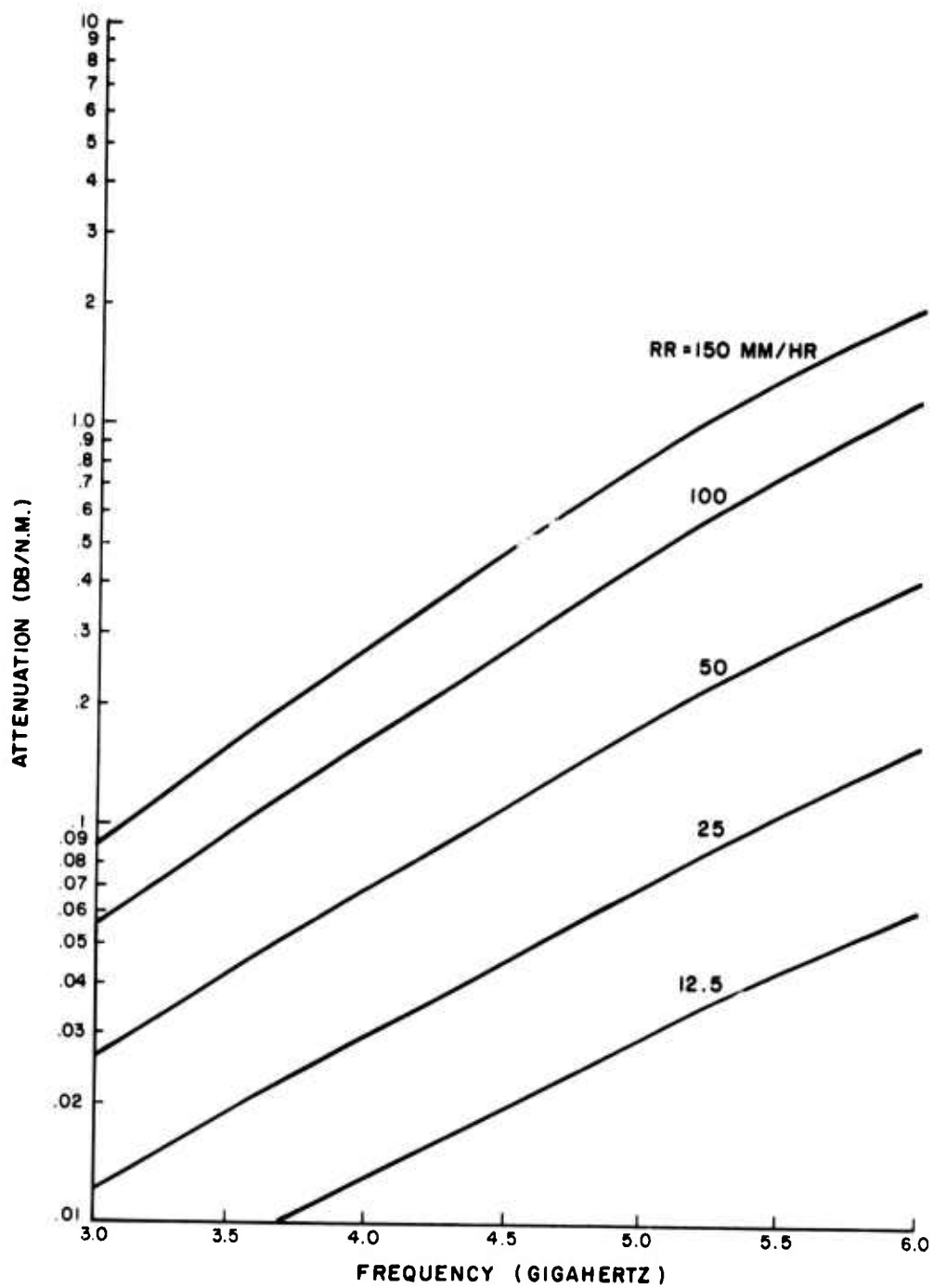


Figure 29.0 ATTENUATION VERSUS FREQUENCY

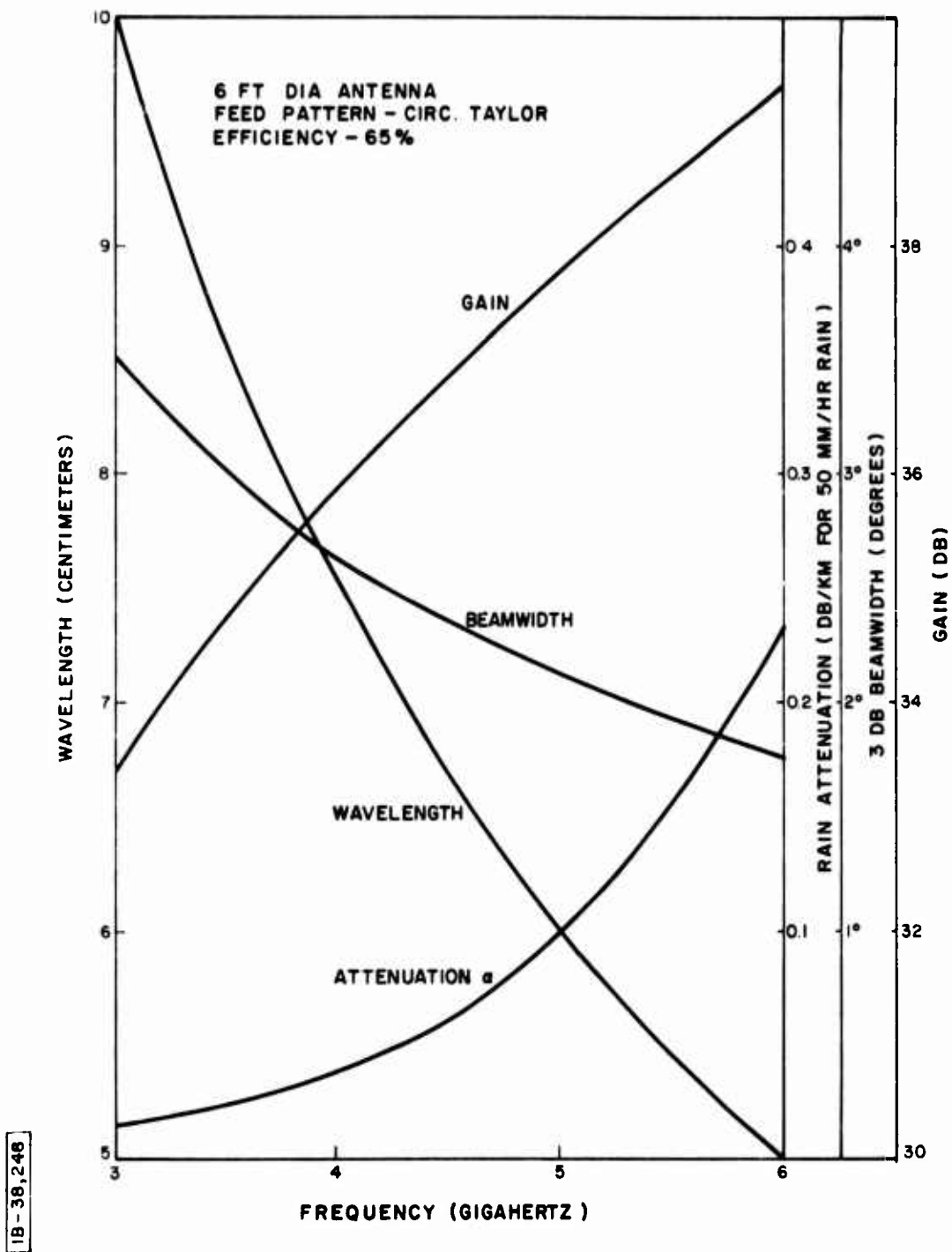


Figure 30.0 ANTENNA CHARACTERISTICS



between 3.1 and 5.5 GHz the attenuation per unit distance increases by a factor of 10, when measured in decibels. To describe the full effect of this, it is necessary to realize that both attenuation and path length appear as exponents in the equation for path loss (L):

$$L = ke^{\alpha x}$$

where: k is a constant and x is the total distance.

This quantity has accordingly been computed for a set of specific examples with the results shown in Figure 31. Here rain rate has been assumed to be constant over a total path length of 100 km (50 km = 28 nautical miles radar range). The loss factor shown is in each case the factor by which transmitter peak power would have to be multiplied in order to obtain the same signal-to-noise ratio at the radar, as would have been the case in the absence of any attenuation. This factor, generally speaking, can be seen to be relatively small at 3000 MHz, moderate to sizeable for 4620 MHz, and very large indeed for 5450 MHz.

The evident non-linearity of attenuation with rain rate is due to differences in drop size distribution for the different rain rates. To illustrate the sensitivity of attenuation to frequency selection further, refer to Figure 32. These curves show attenuation and antenna beamwidth versus frequency for a range interval of 50 nautical miles which is assumed to have a rain rate of 50 mm/hr. Note that as the frequency is decreased from 5450 MHz to 4200 MHz a total round trip attenuation decrease of 18.7 dB is experienced. For the same frequency decrease the antenna beamwidth for a given aperture size (6 feet diameter) increased from  $1.96^\circ$  to  $2.5^\circ$ . This shows that an

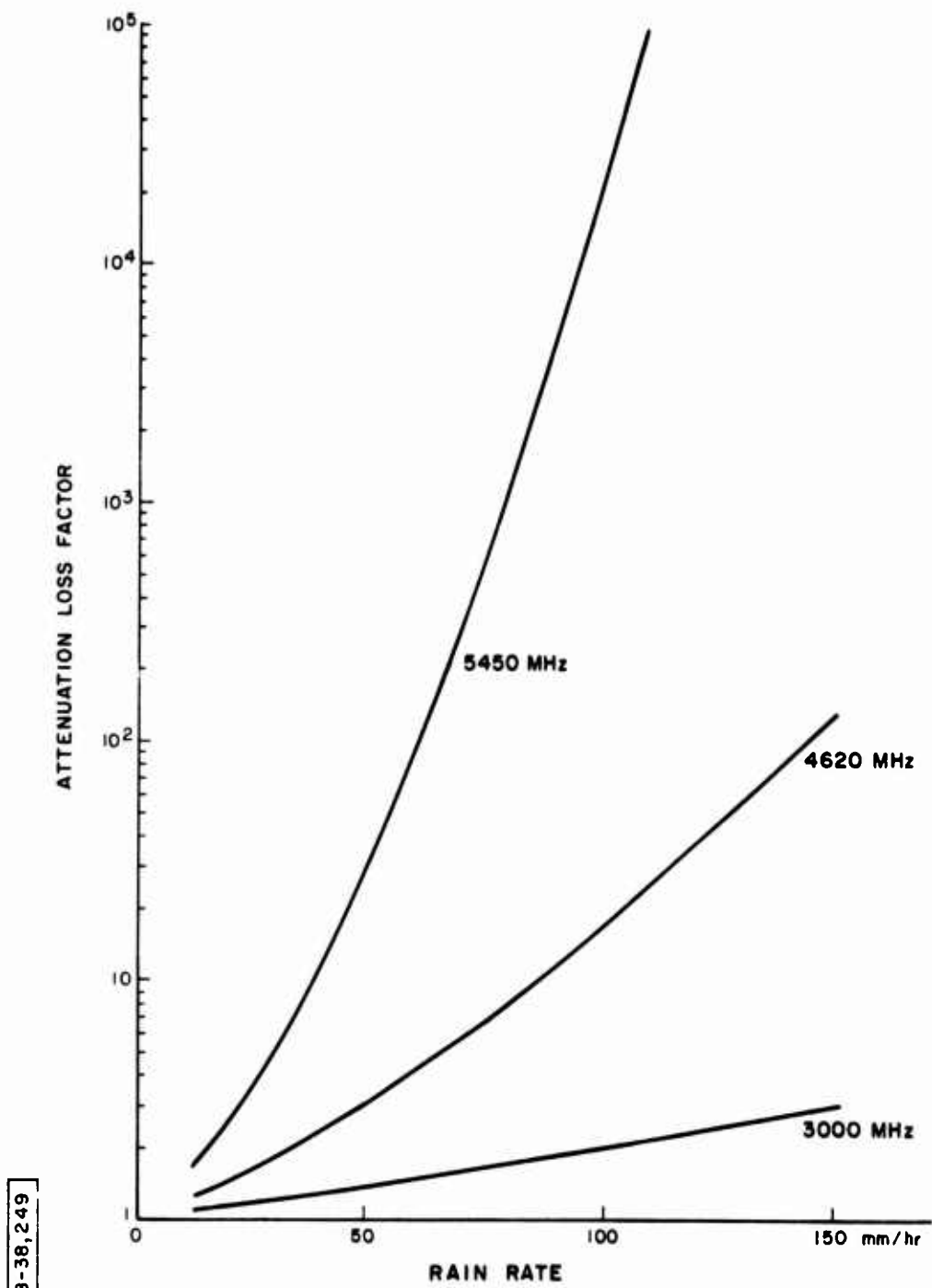


Figure 31.0 ATTENUATION LOSS DUE TO RAIN OVER 100 km PATH LENGTH

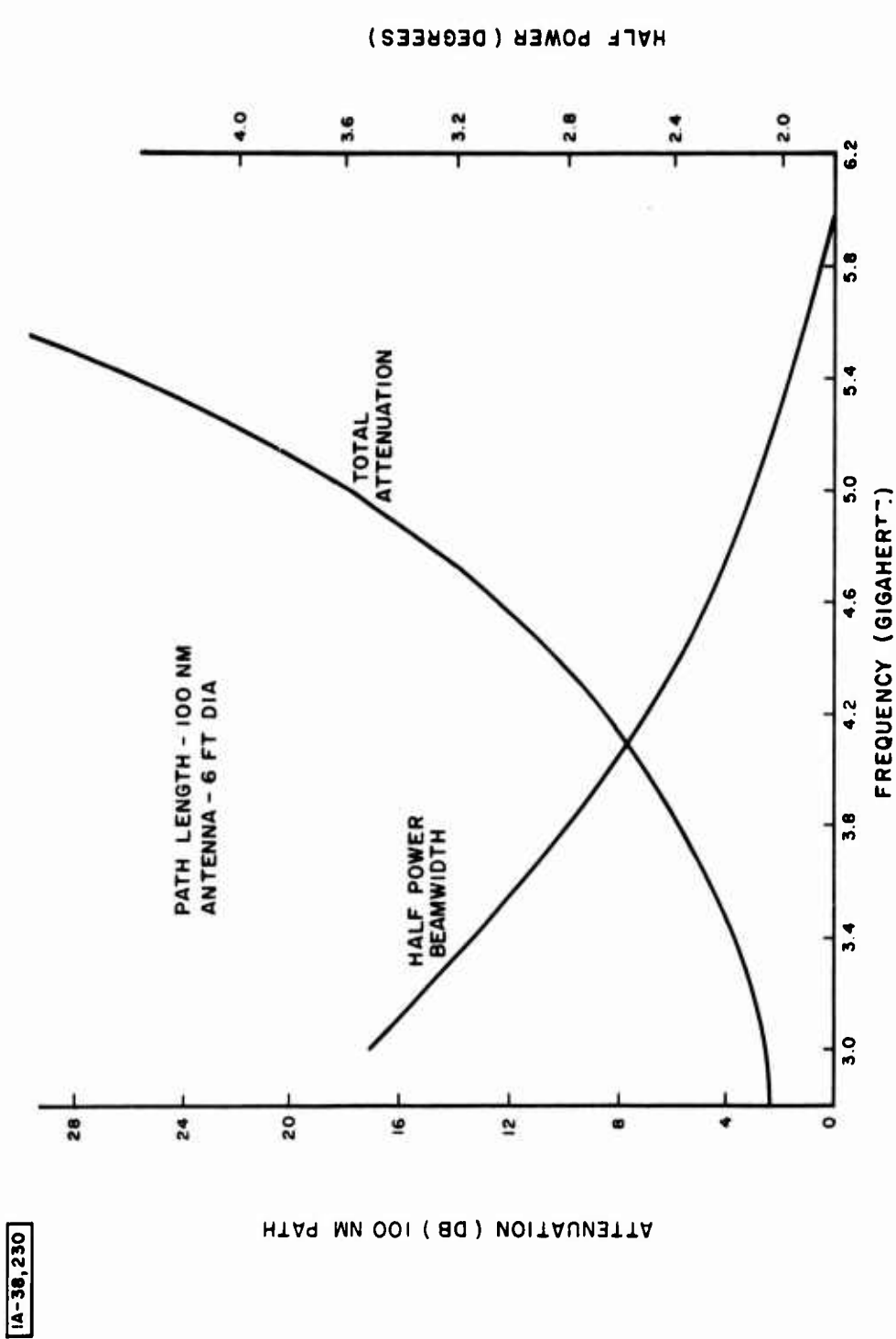


Figure 32.0 TOTAL PATH ATTENUATION AND HALF POWER BEAMWIDTH VERSUS FREQUENCY

increase by a factor of 74 in signal to noise ratio can be achieved while suffering only 27.5% increase in beamwidth by decreasing frequency 23%.

It has also been pointed out<sup>(9)</sup> that even when the beam is fully filled with rain clouds, relatively large errors in rain rate estimates can be encountered with attenuation compensation techniques.

To illustrate how the BFF affects errors in estimating rain intensity at attenuating wavelengths, assume there are two rain bands A and B, which are each 10 nautical miles wide in range as shown in Figure 33. The 3 dB beamwidth (one-way) is assumed to be 2 degrees and the boresight look angle is at  $1^\circ$  elevation above the earth tangent. Assume that both rain bands have a rain rate of 50 mm/hr. The BFF is obtained from the normalized angles  $\phi^+ / \theta_3 = 0$  and  $\phi^- / \theta_3 = -.5$ . From Figure 10 this gives  $BFF^+ = 50\%$  and  $BFF^- = 7\%$ . The total  $BFF = 50 - 7 = 43\%$ , or -3.7 dB. Figure 16 indicates this would represent a rain rate of 56% of true (28 mm/hr) if earth shading compensation is neglected. This is the rain rate which the radar signal would indicate from the reflectivity factor. From Figure 29 it can be seen that attenuation through one nautical mile of 28 mm/hr rain rate at 5000 MHz is 0.08 dB. Therefore, the indicated two-way path attenuation through a 10 nautical mile rainband would be:

$$0.08 \times 10 \times 2 = 1.6 \text{ dB.}$$

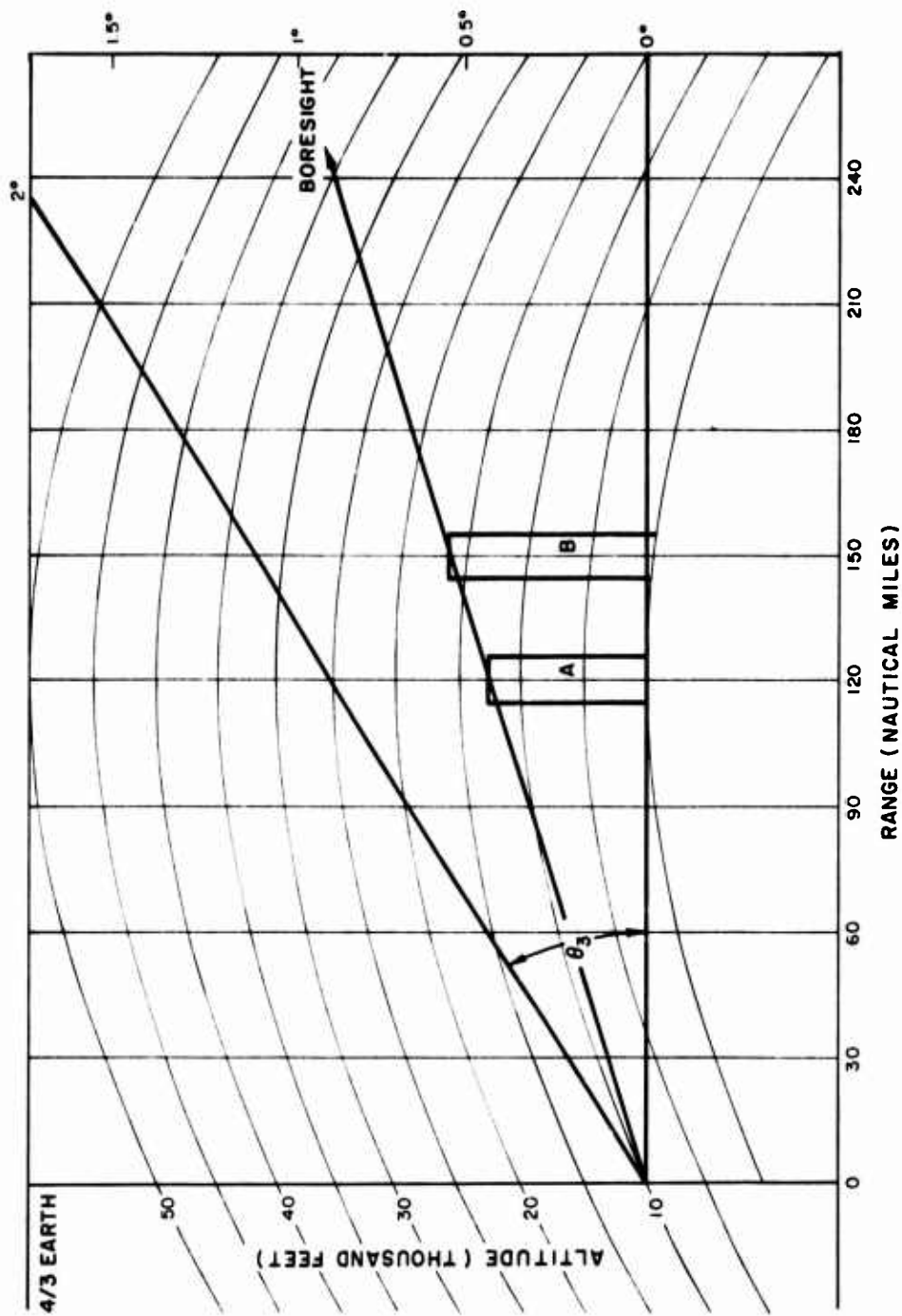


Figure 33.0 AFFECT OF BFF ON RAIN RATE ESTIMATE

Attenuation through 50 mm/hr rain at 5000 MHz is 0.18 dB/NM. Thus the actual attenuation of energy in the lower portion of the beam would be  $0.18 \times 20 = 3.6$  dB.

Now as the beam energy approaches rainband B the BFF is again -3.7 dB and the actual loss in reflectivity is 7.3 dB (3.7 dB BFF loss from rain band B + 3.6 dB attenuation loss through rain band A). The radar can compensate for 1.6 dB of this loss due to radar derived attenuation through an estimated RR of 28 mm/hr. Therefore, the error factor in reflectivity for the radar measurement on the second rainband would be  $-7.3 + 1.6 = -5.7$  dB. From Figure 16 this causes a 40% RR factor or an estimated RR of 20 mm/hr, as opposed to the actual RR of 50 mm/hr. Thus it is obvious that non-beam filling can cause very large errors in rain rate estimates even though estimated attenuation is used to compensate reflectivity measurements.

Since both resolution and rain rate measurements are of concern to the SEEK STORM radar design, it is apparent that a compromise between attenuation affects and resolution will be necessary. To gain an appreciation for this compromise, antenna size and beamwidth at various frequencies will be discussed.

### 3.3.2 Antenna Size

From a practical viewpoint the antenna configuration will be dictated by the ultimate size of radome which can be mounted on the WC-130 aircraft. Preliminary work in this area has indicated the following candidate antenna sizes: 7 feet high (H) by 16 feet wide (W), 5 x 12 feet and 4 x 10 feet. By using Equation 8, Section 2.4 and assuming an efficiency N of 50%, calculations of corresponding antenna gains and azimuth and elevation beamwidth have been performed

for frequencies of 5500, 4400, and 3300 MHz. Results of these calculations are shown in Table III. Note that maximum variation in gain for all cases is 9 dB.

F	H(ft)	W(ft)	G(dB)	$\theta_{AZ}$	$\theta_{E1}$
5500	7	16	44	.8°	1.7°
	5	12	41	1.1	2.3
	4	10	39	1.31	2.9
4400	7	16	42	1.0	2.1
	5	12	40	1.4	2.9
	4	10	38	1.6	3.7
3300	7	16	40	1.4	2.8
	5	12	37	1.8	3.9
	4	10	35	2.2	4.9

TABLE III

#### ANTENNA PARAMETERS

Azimuth beamwidth varies from 0.8 degrees to 2.2 degrees. According to Figure 24 the 3 dB beamwidth should not exceed 1.8 degrees<sup>7</sup> Elevation beamwidths vary from 1.7 to 4.9 degrees. Study of the elevation beamwidth indicate a requirement for not more than 2 degrees and preferably smaller. From this table it appears that a best compromise between attenuation considerations and resolution requirements may be the 7 x 16 foot antenna size operating at a frequency near 4400 MHz.

<sup>7</sup> Assumes:  $\epsilon = .95\theta_{eff}$  and  $\epsilon = 3.8^\circ$

Since;  $\theta_{eff} = 2.24\theta_3$

$$\theta_3 = \frac{3.8}{.95(2.24)} \approx 1.8^\circ$$

### 3.3.3 Transmitter Peak Power

To determine the required transmitter peak power Equation 8 shown in Section 2.5 will be utilized. This equation can be rewritten as:

$$P_T = \frac{S/N R^2 \lambda^2 \theta_A \theta_E L}{\tau^2 Z \bar{K}} \quad (19)$$

where;

$$\bar{K} = \frac{\pi^5 N^2 |K|^2 c}{(8)^2 k T \overline{NF}}$$

and  $\frac{S}{N}$  is the single pulse signal to noise ratio.

The following assumptions will be made:

$S/N = 13$  dB (20:1 ratio),

$\tau = 1$  microsecond

$Z = 7 (10^{15})$  (or  $25 \times 10^{-15}$ )  $m^6/m^3$  (assumes a target cloud of 10 (or 25) mm/hr rain rate at 250 nautical miles range as shown in Figure 9.0),

$N = 50\%$  aperture efficiency,

$|K|^2 = 1$ ,

$k = 1.38 \times 10^{-23}$  watts/ $^\circ K$ /HZ Boltzman's constant,

$\overline{NF} = 7$  dB noise figure,

$T = 300$   $^\circ K$  receiver temperature,

$c = 3 \times 10^8$  meters/sec (velocity of light),

$R = 250$  nautical miles ( $4.63 \times 10^5$  meters),

$L =$  Total losses. (Due to both the radar and the propagation path.  
Radar RF losses assumed to be 3 dB.)



To illustrate how peak power requirement varies the following antenna sizes taken from Table III will be studied:

7 x 16 feet at 5500, 4400, and 3300 MHz

5 x 12 feet at 5500, and 4400 MHz

Calculations of peak power for these five cases have been performed and the results are shown in Table IV. Under columns labeled "no attenuation" only the 3 dB of radar loss is included. Target rain rates of 10 and 25 mm/hr were assumed to consider the effect of attenuation (which varies with frequency) by intervening rain of intensity and extent typical of a severe hurricane. The attenuations resulting from this model are taken into account in the columns of Table IV which are labeled "with Attenuation". These peak power figures are considerably higher and indicate that peak power requirements using C-Band can become very impractical.

CASE	ANTENNA SIZE HxW(FEET)	FREQUENCY MHz	$\theta_A$ DEGREES	$\theta_E$ DEGREES	NO ATTENUATION		WITH ATTENUATION	
					$P_P$ 10 mm/h	$P_P$ 25 mm/h	$P_P$ 10 mm/h	$P_P$ 25 mm/h Target Rain Rate
1	7 x 16	5500	0.8	1.7	86 kW*	24 kW	86 MW*	24 MW
2	5 x 12	5500	1.1	2.3	158 kW	44 kW	158 MW	44 MW
3	7 x 16	4400	1.0	2.1	208 kW	58 kW	3.1 MW	.87 MW
4	5 x 12	4400	1.4	2.9	392 kW	109 kW	.58 MW	1.6 MW
5	7 x 16	3300	1.4	2.8	696 kW	194 kW	1.9 MW	.53 MW

\*MW = MEGAWATT

\*kW = KILOWATT

TABLE IV  
PEAK POWER VARIATIONS

With proper pulse processing a 10 dB lower signal to noise ratio may be usable. If range resolution is sacrificed and a pulse width of perhaps 6 microseconds is used instead of one microsecond this would reduce the peak power by a factor of 36. The above factors combined would reduce the peak power by a factor of 360. Table V shows how the combined signal processing techniques and change in pulse width could alter the peak power requirements, for the condition of full intervening rain attenuation. This table illustrates the large decreases in peak power requirements which can be obtained by parameter and signal processing variations.

REQUIRED PEAK POWER (KILO-WATTS) WITH PARAMETER CHANGES AND SIGNAL PROCESSING				
CASE	ANTENNA SIZE (FEET)	FREQUENCY (MHz)	TO DETECT 10 mm/hr	TO DETECT 25 mm/hr
1	7 x 16	5500	240	66.7
2	5 x 12	5500	440	122
3	7 x 16	4400	8.6	2.4
4	5 x 12	4400	16	4.4
5	7 x 16	3300	5.3	1.5

TABLE V  
PEAK POWER VARIATIONS

#### REFERENCES

- (1) Merrill J. Skolnik, Introduction to Radar, McGraw-Hill, pp. 539-540 and P. 24.
- (2) D. K. Barton, Radar Systems Analysis, Prentice-Hall, P.125.
- (3) Barton and Ward, Handbook of Radar Measurements, Prentice-Hall, 1969, PP 286-287.
- (4) M. F. Girismen, New Sea Clutter Data, ESD-TR-71-166, The MITRE Corporation, Bedford, Massachusetts.
- (5) D. Atlas, "Advances in Radar Meteorology," P. 325 ff., Advances in Geophysics, Vol. 10, Academic Press, New York, 1964.
- (6) F. E. Nathanson, Radar Design Principles, McGraw-Hill, 1969, PP 88-90.
- (7) F. E. Nathanson, J. P. Reilly, Radar Precipitation Echoes," Trans. IEEE, Vol. AES4, #4, July 1968, PP 505-514.
- (8) R. G. Medhurst, Rainfall Attenuation of Centimeter Waves, IEEE Trans. Ant. & Prop., July 1965.
- (9) K. M. Rao, R. W. Shaw, "Attenuation Parameters From a Radar Map," Proc. 13th Meteorological Conference, American Meteorological Society, Boston, Mass., 1968, PP. 504-509.

**Preceding page blank**